Supporting Information

Direct Comparison of (N)-Methanocarba and Ribose-Containing 2-Arylalkynyladenosine Derivatives as A_3 Receptor Agonists

Dilip K. Tosh, Veronica Salmaso, Harsha Rao, Ryan Campbell, Amelia Bitant, Zhan-Guo Gao, John A. Auchampach, Kenneth A. Jacobson

Contents **Pages**

Chemical synthesis

Scheme S1. Synthesis of compounds **16** – **19**. Reagents and conditions: (i) R^1NH_2, Et_3N, MeOH, rt; (ii) R^1NH_2, DIPEA, i-PrOH, 150 °C, MW; (iii) 40% $MeNH_2$, MeOH, rt; (iv) 5-fluoro-2-ethynylthiophene, $PdCl_2(Ph_3P)_2$, CuI, Et_3N, DMF; (v) 10% TFA MeOH, 70 °C.

Scheme S2. Synthesis of compounds **8** and **9**. Reagents and conditions: (i) 5-fluoro-2-ethynylthiophene, $PdCl_2(Ph_3P)_2$, CuI, Et_3N, DMF; (ii) 10% TFA MeOH, 70 °C.

Scheme S3. Synthesis of compound **10**. Reagents and conditions: (i) 1-deaza-2-amino-6-chloro purine, BSA, TMSOTf, CH_3CN, 60 °C; (ii) isoamyl nitrite, CH_2I_2, CuI, I_2, THF, 90 °C; (iii) 40% $MeNH_2$, MeOH, rt; (iv) 2,2-dimethoxy propane, conc. H_2SO_4, acetone, rt (v) TEMPO-BIAB, CH_3CN-H_2O; (vi) $MeNH_2$.HCl, HATU, DIPEA, DMF; (vii) $MeNH_2$.HCl, DIPEA, *i*-PrOH, 150 °C, MW; (viii) 5-fluoro-2-ethynylthiophene, $PdCl_2(Ph_3P)_2$, CuI, Et_3N, DMF; (ix) 10% TFA, MeOH 70 °C.

Scheme S1

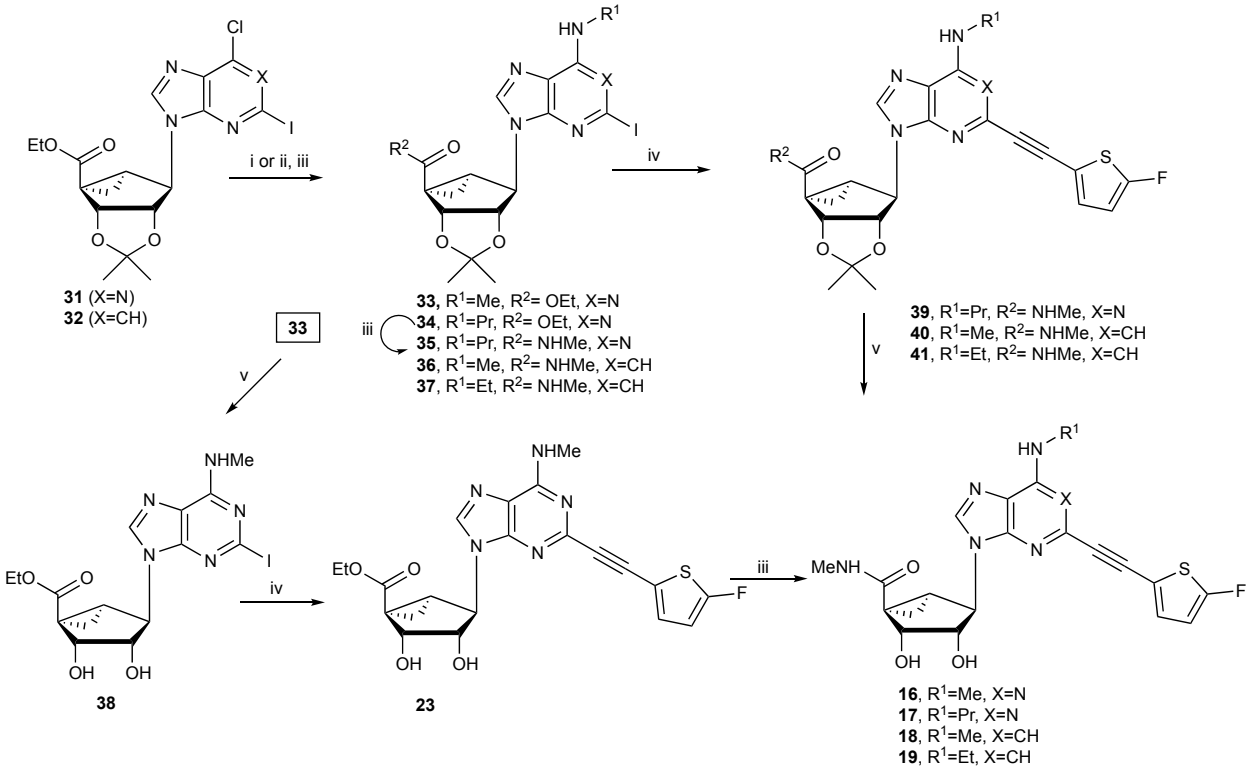

Scheme S2

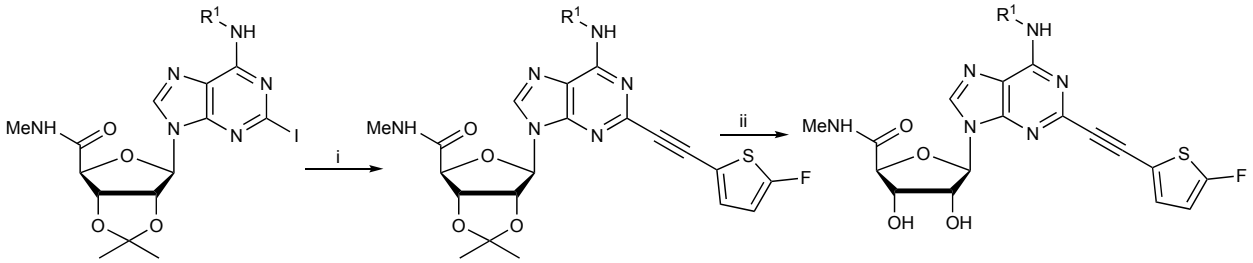

42, R^1=Me
43, R^1=Pr

44, R^1=Me
45, R^1=Pr

8, R^1=Me
9, R^1=Pr

Scheme S3

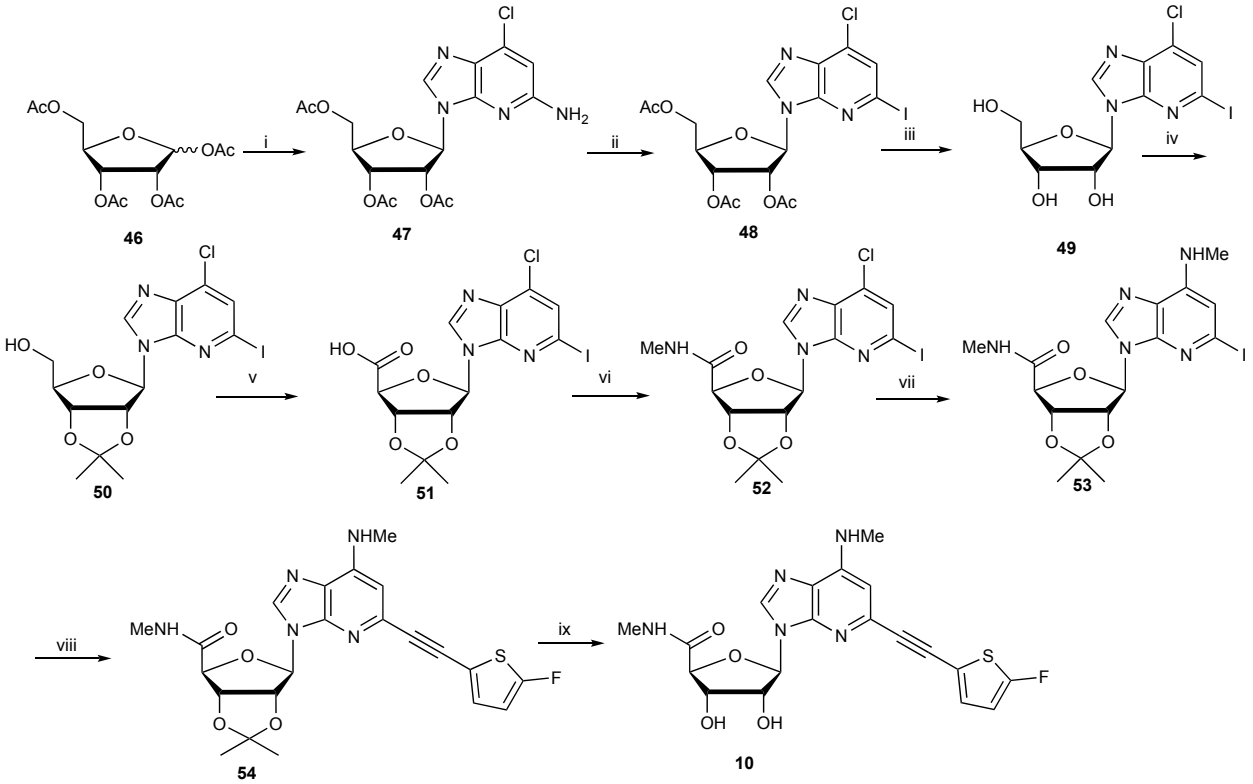

46

47

48

49

50

51

52

53

54

10

Chemical synthesis

Materials and instrumentation

All reagents and solvents were purchased from Sigma-Aldrich (St. Louis, MO). ^{1}H NMR spectra were obtained with a Bruker 400 spectrometer using $CDCl_3$, CD_3OD and DMSO as solvents. Chemical shifts are expressed in δ values (ppm) with tetramethylsilane (δ 0.00) for $CDCl_3$ and water (δ 3.30) for CD_3OD. NMR spectra were collected with a Bruker AV spectrometer equipped with a z-gradient [^{1}H, ^{13}C, ^{15}N]-cryoprobe. TLC analysis was carried out on glass sheets precoated with silica gel F254 (0.2 mm) from Aldrich. The purity of final nucleoside derivatives was checked using a Hewlett−Packard 1100 HPLC equipped with a Zorbax SB-Aq 5 μm analytical column (50 × 4.6 mm; Agilent Technologies Inc., Palo Alto, CA). Mobile phase: linear gradient solvent system, 5 mM TBAP (tetrabutylammonium dihydrogen phosphate) −CH_3CN from 80:20 to 0:100 in 13 min; the flow rate was 0.5 mL/min. Peaks were detected by UV absorption with a diode array detector at 230, 254, and 280 nm. All derivatives tested for biological activity showed >95% purity by HPLC analysis (detection at 254 nm). Low-resolution mass spectrometry was performed with a JEOL SX102 spectrometer with 6-kV Xe atoms following desorption from a glycerol matrix or on an Agilent LC/MS 1100 MSD, with a Waters (Milford, MA) Atlantis C18 column. High resolution mass spectroscopic (HRMS) measurements were performed on a proteomics optimized Q-TOF-2 (Micromass-Waters) using external calibration with polyalanine, unless noted. Observed mass accuracies are those expected based on known performance of the instrument as well as trends in masses of standard compounds observed at intervals during the series of measurements. Reported masses are observed masses uncorrected for this time-dependent drift in mass accuracy. All of the monosubstituted alkyne intermediates were purchased from Sigma-Aldrich (St. Louis, MO), Small Molecules, Inc. (Hoboken, NJ), Anichem (North Brunswick, NJ), PharmaBlock, Inc. (Sunnyvale, CA), Frontier Scientific (Logan, UT) and Tractus (Perrineville, NJ).

(2*S*,3*S*,4*R*,5*R*)-5-(2-((5-Fluorothiophen-2-yl)ethynyl)-6-(methylamino)-9H-purin-9-yl)-3,4-dihydroxy-N-methyltetrahydrofuran-2-carboxamide (8)
Compound **8** (92%) was prepared from compound **44** following the same method as for compound **17**. ^{1}H NMR (CD_3OD, 400 MHz) δ 8.26 (s, 1H), 7.19 (t, *J=4.0* Hz, 1H), 6.65-6.63 (m, 1H), 6.00 (d, *J* = 8.0 Hz, 1H), 4.77-4.74 (m, 1H), 4.50 (1H), 4.33 (d, *J* = 4.8 Hz, 1H), 3.14 (br s, 3H), 3.00 (s, 3H). HRMS calculated for $C_{18}H_{18}N_6O_4FS$ $(M + H)^+$: 433.1094; found 433.1096.

(2*S*,3*S*,4*R*,5*R*)-5-(2-((5-Fluorothiophen-2-yl)ethynyl)-6-(propylamino)-9H-purin-9-yl)-3,4-dihydroxy-*N*-methyltetrahydrofuran-2-carboxamide (9)
Compound **8** (89%) was prepared from compound **45** following the same method as for compound **17**. ^{1}H NMR (CD_3OD, 400 MHz) δ 8.25 (s, 1H), 7.19 (t, *J=4.0* Hz, 1H), 6.65-6.63 (m, 1H), 6.00 (d, *J* = 8.0 Hz, 1H), 4.78-4.75 (m, 1H), 4.50 (s, 1H), 4.33 (dd, J_1 = 1.2 Hz, J_2 = 4.8 Hz, 1H), 3.59 (br s, 2H), 3.00 (s, 3H), 1.77-1.70 (m, 2H), 1.06 (d, *J* = 6.4 Hz, 3H). HRMS calculated for $C_{20}H_{22}N_6O_4FS$ $(M + H)^+$: 461.1407; found 461.1404.

(2*S*,3*S*,4*R*,5*R*)-5-(5-((5-Fluorothiophen-2-yl)ethynyl)-7-(methylamino)-3H-imidazo[4,5-b]pyridin-3-yl)-3,4-dihydroxy-N-methyltetrahydrofuran-2-carboxamide (10)
Compound **10** (92%) was prepared from compound **54** following the same method as for compound **17**. ^{1}H NMR (CD_3OD, 400 MHz) δ 8.32 (br s, 1H), 7.21 (s, 1H), 6.86 (s, 1H), 6.67 (s,

1H), 6.06 (d, *J* = 7.6 Hz, 1H), 4.68-4.61 (m, 2H), 4.28 (d, *J* = 4.4 Hz, 1H), 3.15 (s, 3H), 2.97 (s, 3H). HRMS calculated for $C_{19}H_{19}N_5O_4FS$ $(M + H)^+$: 432.1142; found 432.1141.

(1*S*,2*R*,3*S*,4*R*,5*S*)-4-(2-((5-Fluorothiophen-2-yl)ethynyl)-6-(methylamino)-9H-purin-9-yl)-2,3-dihydroxy-*N*-methylbicyclo[3.1.0]hexane-1-carboxamide (16)

40% $MeNH_2$ (1.5 mL) solution was added to a solution of compound **23** (50 mg, 0.1 mmol) in MeOH (1.5 mL) and stirred at room temperature for overnight. Solvent was evaporated and the residue was purified on flash silica gel column chromatography (CH_2Cl_2:MeOH = 20:1) to give the compound **16** (36 mg, 75%) as a colorless syrup. ^{1}H NMR (CD_3OD, 400 MHz) δ 8.09 (s, 1H), 7.19 (t, *J* = 4.0 Hz, 1H), 6.64-6.62 (m, 1H), 5.05 (d, *J* = 6.4 Hz, 1H), 4.81 (s, 1H), 4.02 (d, *J* = 6.4 Hz, 1H), 3.13 (br s, 3H), 2.12-2.09 (m, 1H), 1.88 (t, *J* = 4.8 Hz, 1H), 1.41-1.38 (m, 1H). HRMS calculated for $C_{20}H_{20}N_6O_3FS$ $(M + H)^+$: 443.1302; found 443.1295.

(1*S*,2*R*,3*S*,4*R*,5*S*)-4-(2-((5-Fluorothiophen-2-yl)ethynyl)-6-(propylamino)-9H-purin-9-yl)-2,3-dihydroxy-*N*-methylbicyclo[3.1.0]hexane-1-carboxamide (17)

A solution of compound **39** (36 mg, 0.07 mmol) in methanol (1.5 mL) and 10% trifluoromethanesulfonic acid (1.5 mL) was heated at 70 °C for 3 h. Solvent was evaporated under vacuum, and the residue was purified on flash silica gel column chromatography (CH_2Cl_2:MeOH = 30:1) to give the compound **17** (30 mg, 91%) as colorless syrup. ^{1}H NMR (CD_3OD, 400 MHz) δ 8.10 (s, 1H), 7.19 (t, *J* = 4.0 Hz, 1H), 6.64-6.62 (m, 1H), 5.04 (d, *J* = 6.4 Hz, 1H), 4.82 (s, 1H), 4.02 (d, *J* = 6.4 Hz, 1H), 3.57 (br s, 2H), 2.86 (s, 3H), 2.12-2.09 (m, 1H), 1.88 (t, *J* = 4.8 Hz, 1H), 1.75-1.68 (m, 2H), 1.41-1.37 (m, 1H), 1.04 (t, *J* = 7.2 Hz, 3H). HRMS calculated for $C_{22}H_{24}N_6O_3FS$ $(M + H)^+$: 471.1615; found 471.1623.

(1*S*,2*R*,3*S*,4*R*,5*S*)-4-(5-((5-Fluorothiophen-2-yl)ethynyl)-7-(methylamino)-3H-imidazo[4,5-b]pyridin-3-yl)-2,3-dihydroxy-N-methylbicyclo[3.1.0]hexane-1-carboxamide (18)

Compound **18** (91%) was prepared from compound **40** following the same method as for compound **17**. ^{1}H NMR (CD_3OD, 400 MHz) δ 8.35 (s, 1H), 7.13 (t, *J* = 4.0 Hz, 1H), 6.71 (s, 1H), 6.63-6.61 (m, 1H), 4.98 (d, *J* = 6.0 Hz, 1H), 4.93 (s, 1H), 4.01 (d, *J* = 6.4 Hz, 1H), 3.07 (s, 3H), 2.86 (s, 3H), 2.15-2.11 (m, 1H), 1.92 (t, *J* = 4.8 Hz, 1H), 1.42-1.38 (m, 1H). HRMS calculated for $C_{21}H_{21}N_5O_3FS$ $(M + H)^+$: 442.1349 Found 442.1349.

(1*S*,2*R*,3*S*,4*R*,5*S*)-4-(7-(Ethylamino)-5-((5-fluorothiophen-2-yl)ethynyl)-3H-imidazo[4,5-b]pyridin-3-yl)-2,3-dihydroxy-N-methylbicyclo[3.1.0]hexane-1-carboxamide (19)

Compound **19** (90%) was prepared from compound **41** following the same method as for compound **17**. ^{1}H NMR (CD_3OD, 400 MHz) δ 8.41 (s, 1H), 7.14 (t, *J* = 4.0 Hz, 1H), 6.74 (s, 1H), 6.63-6.61 (m, 1H), 4.98 (d, *J* = 6.4 Hz, 1H), 4.94 (s, 1H), 4.01 (d, *J* = 6.0 Hz, 1H), 3.51-3.46 (m, 2H), 2.86 (s, 3H), 2.15-2.12 (m, 1H), 1.92 (t, *J* = 4.8 Hz, 1H), 1.42-1.34 (m, 4H). HRMS calculated for $C_{22}H_{23}N_5O_3FS$ $(M + H)^+$: 456.1506; found 456.1508.

Ethyl (1*S*,2*R*,3*S*,4*R*,5*S*)-4-(2-((5-Fluorothiophen-2-yl)ethynyl)-6-(methylamino)-9H-purin-9-yl)-2,3-dihydroxybicyclo[3.1.0]hexane-1-carboxylate (23)

Compound **23** (84%) was prepared from compound **38** following the same method for compound 3**9**. ^{1}H NMR (CD_3OD, 400 MHz) δ 8.04 (s, 1H), 7.20 (t, *J* = 4.0 Hz, 1H), 6.64-6.62 (m, 1H), 5.22 (d, *J* = 6.4 Hz, 1H), 4.84 (s, 1H), 4.27-4.22 (m, 2H), 4.12 (d, *J* = 6.8 Hz, 1H), 3.13 (br s, 3H),

2.23-2.19 (m, 1H), 1.92 (t, *J* = 4.8 Hz, 1H), 1.67-1.63 (m, 1H), 1.29 (t, *J* = 7.2 Hz, 3H). HRMS calculated for $C_{21}H_{21}N_5O_4FS$ $(M + H)^+$: 458.1298; found 458.1298.

Ethyl (3a*R*,3b*S*,4a*S*,5*R*,5a*S*)-5-(2-((5-fluorothiophen-2-yl)ethynyl)-6-(propylamino)-9H-purin-9-yl)-2,2-dimethyltetrahydrocyclopropa[3,4]cyclopenta[1,2-d][1,3]dioxole-3b(3aH)-carboxylate (39)

$PdCl_2(PPh_3)_2$ (12.32 mg, 0.01 mmol), CuI (1.6 mg, 0.008 mmol), 2-ethynyl-5-fluorothiophene (66 mg, 0.52 mmol) and triethylamine (0.12 mL, 0.87 mmol) were added to a solution of compound **35** (45 mg, 0.08 mmol) in anhydrous DMF (1.0 mL), and the mixture heated at 66 ^oC for 2 h. Solvent was evaporated under vacuum, and the residue was purified on flash silica gel column chromatography (CH_2Cl_2:MeOH = 35:1) to give the compound **39** (36 mg, 82%) as a brown syrup. ^1H NMR (CD_3OD, 400 MHz) δ 8.14 (s, 1H), 7.25 (t, *J* = 4.0 Hz, 1H), 6.64-6.63 (m, 1H), 5.80 (d, *J* = 7.2 Hz, 1H), 5.01 (s, 1H), 3.57 (br s, 2H), 2.82 (s, 3H), 2.16-2.13 (m, 1H), 1.75-1.71 (m, 2H), 1.55 (s, 3H), 1.42 (t, *J* = 5.2 Hz, 1H), 1.31 (s, 3H), 1.03 (t, *J* = 7.2 Hz, 3H). HRMS calculated for $C_{25}H_{28}N_6O_3FS$ $(M + H)^+$: 511.1928; found 511.1929.

(3a*R*,3b*S*,4a*S*,5*R*,5a*S*)-5-(5-((5-Fluorothiophen-2-yl)ethynyl)-7-(methylamino)-3H-imidazo[4,5-b]pyridin-3-yl)-N,2,2-trimethyltetrahydrocyclopropa[3,4]cyclopenta[1,2-d][1,3]dioxole-3b(3aH)-carboxamide (40)

Compound **40** (82%) was prepared from compound **36** following the same method as for compound 3**9**. ^1H NMR (CD_3OD, 400 MHz) δ 8.17 (s, 1H), 7.15 (t, *J* = 4.0 Hz, 1H), 6.63 (s, 1H), 6.61-6.60 (m, 1H), 5.77 (d, *J* = 6.8 Hz, 1H), 5.05 (s, 1H), 4.85 (d, *J* = 6.4 Hz, 1H), 3.00 (s, 3H), 2.81 (s, 3H), 2.15-2.11 (m, 1H), 1.56-1.53 (m, 4H), 1.42 (t, *J* = 5.2 Hz, 1H), 1.29 (s, 3H). HRMS calculated for $C_{24}H_{25}N_5O_3FS$ $(M + H)^+$: 482.1662; found 482.1667.

(3a*R*,3b*S*,4a*S*,5*R*,5a*S*)-5-(7-(Ethylamino)-5-((5-fluorothiophen-2-yl)ethynyl)-3H-imidazo[4,5-b]pyridin-3-yl)-N,2,2-trimethyltetrahydrocyclopropa[3,4]cyclopenta[1,2-d][1,3]dioxole-3b(3aH)-carboxamide (41)

Compound **41** (81%) was prepared from compound **37** following the same method for compound 3**9**. ^1H NMR (CD_3OD, 400 MHz) δ 8.15 (s, 1H), 7.15 (t, *J* = 4.0 Hz, 1H), 6.67 (s, 1H), 6.62-6.60 (m, 1H), 5.77 (d, *J* = 6.8 Hz, 1H), 5.05 (s, 1H), 4.85 (d, *J* = 6.4 Hz, 1H), 3.44-3.39 (m, 2H), 2.82 (s, 3H), 2.15-2.11 (m, 1H), 1.56-1.53 (m, 4H), 1.42 (t, *J* = 5.2 Hz, 1H), 1.34 (t, *J* = 7.2 Hz, 3H), 1.29 (s, 3H). HRMS calculated for $C_{25}H_{27}N_5O_3FS$ $(M + H)^+$: 496.1819; found 496.1826.

(3a*S*,4*S*,6*R*,6a*R*)-6-(2-((5-Fluorothiophen-2-yl)ethynyl)-6-(methylamino)-9H-purin-9-yl)-N,2,2-trimethyltetrahydrofuro[3,4-d][1,3]dioxole-4-carboxamide (44)

Compound **44** (80%) was prepared from compound **42** following the same method as for compound 3**9**. ^1H NMR (CD_3OD, 400 MHz) δ 8.21 (s, 1H), 7. 23 (t, *J* = 4.0 Hz, 1H), 6.63 (t, *J* = 4.0 Hz, 1H), 6.31 (d, *J* = 1.6, 1H), 5.51 (d, *J* = 4.0 Hz, 1H), 5.38 (d, *J* = 4.0 Hz, 1H), 4.66 (s, 1H), 3.12 (br s, 3H), 2.53 (s, 3H), 1.62 (s, 3H), 1.42 (s, 3H). HRMS calculated for $C_{21}H_{22}N_6O_4FS$ $(M + H)^+$: 473.1407; found 473.1411.

(3a*S*,4*S*,6*R*,6a*R*)-6-(2-((5-Fluorothiophen-2-yl)ethynyl)-6-(propylamino)-9H-purin-9-yl)-N,2,2-trimethyltetrahydrofuro[3,4-d][1,3]dioxole-4-carboxamide (45)

Compound **45** (82%) was prepared from compound **43** following the same method as for compound 3**9**. ^1H NMR (CD_3OD, 400 MHz) δ 8.21 (s, 1H), 7.22 (t, *J* = 4.0 Hz, 1H), 6.63-6.64

(m, 1H), 6.30 (s, 1H), 4.66 (s, 1H), 3.56 (br s, 2H), 2.53 (s, 3H), 1.75-1.62 (m, 2H), 1.62 (s, 3H), 1.42 (s, 3H), 1.03 (t, J = 7.6 Hz, 3H). HRMS calculated for $C_{23}H_{26}N_6O_4FS$ $(M + H)^+$: 501.1720; found 501.1723.

(2*R*,3*R*,4*R*,5*R*)-2-(Acetoxymethyl)-5-(5-amino-7-chloro-3H-imidazo[4,5-b]pyridin-3-yl)tetrahydrofuran-3,4-diyl diacetate (47)

BSA (0.76 mL, 3.14 mmol) was added to a suspension of 1-deaza-2-amino-6-chloro-purine (317 mg, 1.88 mmol) in dry CH_3CN (35 mL) and heated at 60 ^oC for 1 h until it became clear. A solution of tetraacetate riboside (500 mg, 1.57 mmol) in dry CH_3CN (10 mL) followed by TMSOTf (0.14 mL, 0.78 mmol) were added into the reaction mixture and continued heating at 60 ^oC for overnight. The reaction mixture was cooled down to room temperature and quenched with saturated $NaHCO_3$ solution and stirred for 15 min. Aqueous layer was extracted with ethyl acetate (3 times) and combined organic layer was washed with brine, filtered and evaporated. The residue was purified on flash silica gel column chromatography (hexane:ethyl acetate = 1:2) to give the compound **48** (445 mg, 66%) as foamy solid. ^1H NMR (CD_3OD, 400 MHz) δ 8.12 (s, 1H), 6.61 (s, 1H), 6.18 (d, J = 4.4 Hz, 1H), 6.06 (t, J = 5.2 Hz, 1H), 5.86 (t, J = 5.2 Hz, 1H), 4.48-4.47 (m, 1H), 4.44-4.35 (m, 2H), 2.14 (s, 3H), 2.08 (s, 3H), 2.03 (s, 3H). HRMS calculated for $C_{17}H_{20}N_4O_7Cl$ $(M + H)^+$: 427.1021; found 427.1016.

(2*R*,3*R*,4*R*,5*R*)-2-(Acetoxymethyl)-5-(7-chloro-5-iodo-3H-imidazo[4,5-b]pyridin-3-yl)tetrahydrofuran-3,4-diyl diacetate (48)

CuI (218 mg, 1.14 mmol), iodine (264 mg, 1.04 mmol), CH_2I_2 (0.84 mL, 10.4 mmol) and isoamyl nitrite (0.42 mL, 3.13 mmol) were added to a solution of compound **47** (445 mg, 1.04 mmol) in dry THF (15 mL) and refluxed at 90 ^oC for 2 h. After cooling down the reaction mixture to room temperature, water was added into the reaction mixture and the aqueous layer was extracted with ethyl acetate. The combined organic layer was washed with saturated sodium bisulfite solution followed by brine, dried, filtered and evaporated under vacuum. The residue was purified on flash silica gel column chromatography (hexane:ethyl acetate = 2:1) to give the compound **48** (296 mg, 53%) as a brownish syrup. ^1H NMR (CD_3OD, 400 MHz) δ 8.54 (s, 1H), 7.87 (s, 1H), 6.32 (d, J = 4.8 Hz, 1H), 5.98 (t, J = 5.2 Hz, 1H), 5.76 (t, J = 5.2 Hz, 1H), 4.48-4.38 (m, 3H), 2.16 (s, 3H), 2.10 (s, 3H), 2.06 (s, 3H).HRMS calculated for $C_{17}H_{18}N_3O_7ClI$ $(M + H)^+$: 537.9878; found 537.9875.

(2*R*,3*R*,4*S*,5*R*)-2-(7-Chloro-5-iodo-3H-imidazo[4,5-b]pyridin-3-yl)-5-(hydroxymethyl) tetrahydrofuran-3,4-diol (49)

A solution of compound **48** (142 mg, 0.26 mmol) in MeOH (4 mL) and 40% $MeNH_2$ (4 mL) were stirred at room temperature for 5 h. Solvent was evaporated and the residue was purified on flash silica gel chromatography (CH_2Cl_2:MeOH = 15:1) to give the compound **49** (91 mg, 84%) as a colorless syrup. ^1H NMR (CD_3OD, 400 MHz) δ 8.70 (s, 1H), 7.86 (s, 1H), 6.12 (d, J = 5.6 Hz, 1H), 4.71 (d, J = 5.2 Hz, 1H), 4.38 (t, J = 8.8 Hz, 1H), 4.18-4.15 (m, 1H), 4.93 (dd, J_1 = 3.2 Hz, J_2 = 12.4 Hz, 1H), 3.81 (dd, J_1 = 3.2 Hz, J_2 = 12.4 Hz, 1H). HRMS calculated for $C_{11}H_{12}N_3O_4ClI$ $(M + H)^+$: 411.9483; found 411.9487.

((3a*R*,4*R*,6*R*,6a*R*)-6-(7-Chloro-5-iodo-3H-imidazo[4,5-b]pyridin-3-yl)-2,2-dimethyltetra hydrofuro[3,4-d][1,3]dioxol-4-yl)methanol (50)

2,2-Dimethoxypropane (0.2 mL, 1.65 mmol) and conc. H_2SO_4 (10.2 µL), were added to a solution of compound **49** (68 mg, 0.16 mmol) in acetone (2 mL) and stirred at room temperature for overnight. Reaction mixture was neutralized with $NaHCO_3$ and evaporated under vacuum. The residue was partition with water and ethyl acetate, the combined organic layer was dried, filtered and evaporated. The residue was purified on flash silica gel column chromatography (hexane:ethyl acetate = 1:2) to give the compound **50** (55 mg, 74%) as a colorless syrup. ^{1}H NMR (CD_3OD, 400 MHz) δ 8.66 (s, 1H), 7.86 (s, 1H), 6.29 (d, J = 6.4 Hz, 1H), 5.36-5.33 (m, 1H), 5.07-5.03 (m, 1H), 4.41-4.36 (m, 1H), 3.82-3.72 (m, 2H), 1.63 (s, 3H), 1.41 (s, 3H). HRMS calculated for $C_{14}H_{16}N_3O_4ClI$ $(M + H)^+$: 451.9874; found 451.9870.

(3a*S*,4*S*,6*R*,6a*R*)-6-(7-Chloro-5-iodo-3H-imidazo[4,5-b]pyridin-3-yl)-2,2-dimethyltetrahydro furo[3,4-d][1,3]dioxole-4-carboxylic acid (51)

TEMPO (19 mg, 0.24 mmol), BAIB (98 mg, 0.3 mmol) were added to a solution of compound **50** (55 mg, 0.12 mmol) in CH_3CN (1 mL) and water (1 mL) and stirred at room temperature for 2 days. Aqueous layer was extracted with ethyl acetate (3 times) and the combined organic layer was dried, filtered and evaporated. The residue was purified on flash silica gel column chromatography (CH_2Cl_2:MeOH = 15:1) to give the compound **51** (28 mg, 50%) as a colorless syrup. ^{1}H NMR (CD_3OD, 400 MHz) δ 8.57 (s, 1H), 7.80 (s, 1H), 6.43 (s, 1H), 5.68 (d, J = 5.6 Hz, 1H), 5.57 (d, J = 6.0 Hz, 1H), 4.79 (s, 1H), 1.60 (s, 3H), 1.44 (s, 3H). HRMS calculated for $C_{14}H_{14}N_3O_5ClI$ $(M + H)^+$: 465.9667; found 465.9665.

(3a*S*,4*S*,6*R*,6a*R*)-6-(7-chloro-5-iodo-3H-imidazo[4,5-b]pyridin-3-yl)-N,2,2-trimethyltetrahydrofuro[3,4-d][1,3]dioxole-4-carboxamide (52)

$MeNH_2$.HCl (4.8 mg, 0.072 mmol), HATU (29.7 mg, 0.078 mmol) and DIPEA (13 µL, 0.078 mmol) were added to a solution of compound **51** (28 mg, 0.06 mmol) in DMF (1 mL) and stirred at room temperature for overnight. Solvent was evaporated under vacuum and the residue was purified on flash silica gel column chromatography (hexane:ethyl acetate = 1:3) to give the compound **52** (26 mg, 93%) as colorless syrup. ^{1}H NMR (CD_3OD, 400 MHz) δ 8.54 (s, 1H), 7.83 (s, 1H), 6.44 (s, 1H), 5.64-5.62 (dd, J_1 = 2.4 Hz, J_2 = 6.2 Hz, 1H), 5.47 (d, J = 6.4 Hz, 1H), 4.69 (s, 1H), 2.35 (d, J = 4.8 Hz, 3H), 1.61 (s, 3H), 1.42 (s, 3H). HRMS calculated for $C_{15}H_{17}N_4O_4ClI$ $(M + H)^+$: 478.9983; found 478.9978.

(3a*S*,4*S*,6*R*,6a*R*)-6-(5-Iodo-7-(methylamino)-3H-imidazo[4,5-b]pyridin-3-yl)-N,2,2-trimethyltetrahydrofuro[3,4-d][1,3]dioxole-4-carboxamide (53)

To a solution of compound **52** (33 mg, 0.069 mmol) in DMF (1 mL) $MeNH_2$.HCl (23.2 mg, 0.34 mmol) and DIPEA (0.12 mL, 0.69 mmol) were heated at 150 ^{o}C for 3 h under microwave condition. Solvent was evaporated under vacuum and the residue was purified on flash silica gel column chromatography (Ethyl acetate:MeOH = 60:1) to give the compound **53** (21 mg, 65%) as colorless syrup. ^{1}H NMR (CD_3OD, 400 MHz) δ 8.08 (s, 1H), 6.75 (s, 1H), 6.30 (s, 1H), 5.57 (d, J = 5.6 Hz, 1H), 5.41 (d, J = 5.6 Hz, 1H), 4.62 (s, 1H), 2.97 (s, 3H), 2.43 (s, 3H), 1.60 (s, 3H), 1.41 (s, 3H). HRMS calculated for $C_{16}H_{21}N_5O_4I$ $(M + H)^+$: 474.0638; found 474.0642.

(3a*S*,4*S*,6*R*,6a*R*)-6-(5-((5-Fluorothiophen-2-yl)ethynyl)-7-(methylamino)-3H-imidazo[4,5-b]pyridin-3-yl)-N,2,2-trimethyltetrahydrofuro[3,4-d][1,3]dioxole-4-carboxamide (54)

$PdCl_2(PPh_3)_2$ (6.22 mg, 0.008 mmol), CuI (1.0 mg, 0.004 mmol), 2-ethynyl-5-fluorothiophene (34 mg, 0.52 mmol) and triethylamine (61 µL, 0.44 mmol) were added to a solution of

compound **53** (21 mg, 0.044 mmol) in anhydrous DMF (1.0 mL), and the mixture heated at 70 ^{o}C for 2 h. Solvent was evaporated under vacuum, and the residue was purified on flash silica gel column chromatography (CH_2Cl_2:MeOH = 45:1) to give the compound **54** (17 mg, 84%) as a brown syrup. ^{1}H NMR (CD_3OD, 400 MHz) δ 8.22 (s, 1H), 7.68-7.63 (m, 1H), 7.59-7.55 (m, 1H), 7.12 (t, *J* = 4.0 Hz, 1H), 6.65 (s, 1H), 6.60 (t, *J* = 3.6 Hz, 1H), 6.30 (d, *J* = 6.0 Hz, 1H), 5.45-5.39 (m, 2H), 4.65 (s, 1H), 3.03 (s, 3H), 2.56 (s, 3H), 1.63 (s, 3H), 1.41 (s, 3H). HRMS calculated for $C_{22}H_{23}N_5O_4FS$ $(M + H)^{+}$: 472.1455; found 472.1464.

Pharmacological Methods

The nucleoside analogues were examined in radioligand binding assays (Table 1A and 1B) at three hARs and two or three mARs as previously described.[1-3]

Binding affinity for human A_1AR, $A_{2A}AR$, and A_3ARs was measured as described using membranes from human embryonic kidney (HEK)-293 HEK293 (hA_1AR, $hA_{2A}AR$) or CHO (hA_3AR) stably expressing individual recombinant mouse adenosine receptors and using the agonists radioligands. The binding affinity for hA_1, A_{2A} and A_3ARs was expressed as K_i values using agonists [^{3}H]*N*^{6}-R-phenylisopropyladenosine **55**, [^{3}H]2-[p-(2-carboxyethyl)phenyl-ethylamino]-5′-*N*-ethylcarboxamidoadenosine **56**, or [^{125}I]*N*^{6}-(4-amino-3-iodobenzyl)adenosine-5′-*N*-methyluronamide **57**, respectively. A percent in italics refers to inhibition of binding at 10 μM. Nonspecific binding was determined using 10 μM adenosine 5′-*N*-ethyluronamide **58** or *N*-(2-aminoethyl)-2-[4-(2,3,6,7-tetrahydro-2,6-dioxo-1,3-dipropyl-1*H*-purin-8-yl)phenoxy]-acetamide (XAC, **59**, hA_1AR, $hA_{2A}AR$.

Binding affinity for mouse A_1AR, $A_{2A}AR$, and A_3ARs was measured as described[4] using membranes from human embryonic kidney (HEK)-293 cells stably expressing individual recombinant mouse adenosine receptors and using the agonists [^{125}I]*N*^{6}-(4-amino-3-iodobenzyl)adenosine-5'-methyluronamide ([^{125}I]AB-MECA; A_1AR and A_3AR) and [^{3}H]CGS21680 ($A_{2A}AR$) as radioligands. Nonspecific binding was defined using 100 μM adenosine-5'-*N*-ethylcarboxamide (NECA).

K_i values were obtained using the Cheng-Prusoff equation[5] from IC_{50} values calculated by non-linear regression analysis of specific binding data using GraphPad Prism software (San Diego, CA). In cases where there was only ~50% AR binding inhibition at 10 μM, an estimated K_i of ~10 μM was used in approximating the selectivity ratio.

For one compound, activation of the Gs-coupled human $A_{2B}AR$ stably expressed in CHO cells was measured as described.[6]

References:

1. Carlin, J. L.; Jain, S.; Gizewski, E.; Wan, T. C.; Tosh, D. K.; Xiao, C.; Auchampach, J. A.; Jacobson, K. A.; Gavrilova, O.; Reitman, M. L. Hypothermia in mouse is caused by adenosine A_1 and A_3 receptor agonists and AMP via three distinct mechanisms. *Neuropharmacology* **2017**, *114*, 101–113.

2. Tosh, D. K.; Paoletta, S.; Deflorian, F.; Phan, K.; Moss, S. M.; Gao, Z. G.; Jiang, X.; Jacobson, K. A. Structural sweet spot for A_1 adenosine receptor activation by truncated (N)-methanocarba nucleosides: Receptor docking and potent anticonvulsant activity. *J. Med. Chem.* **2012**, *55*, 8075–8090.

3. Tosh, D. K.; Ciancetta, A.; Warnick, E.; Crane, S.; Gao, Z. G.; Jacobson, K. A. Structure-based scaffold repurposing for G protein-coupled receptors: Transformation of adenosine derivatives into $5HT_{2B}$/$5HT_{2C}$ serotonin receptor antagonists. *J. Med. Chem.* **2016**, *59*, 11006–11026.

4. Kreckler, L.M.; Wan, T.C.; Ge, Z.D.; Auchampach, J.A. Adenosine inhibits tumor necrosis factor-alpha release from mouse peritoneal macrophages via A_{2A} and A_{2B} but not the A_3 adenosine receptor. *J. Pharmacol. Exp. Ther.* **2006**, *317* (1), 172e180.

5. Cheng, Y. C.; Prusoff, W. H. Relationship between the inhibition constant (K_I) and the concentration of inhibitor which causes 50 per cent inhibition (I_{50}) of an enzymatic reaction. *Biochem. Pharmacol.* **1973**, *22*, 3099–3108.

6. Jacobson, K.A.; Ohno, M.; Duong, H.T.; Kim, S.K.; Tchilibon, S.; Cesnek, M.; Holy, A.; Gao, Z.G. A neoceptor approach to unraveling microscopic interactions between the human A_{2A} adenosine receptor and its agonists. *Chemistry and Biology* **2005**, *12*, 237-247.

Table S1. PDSP Off-target screening (human, unless noted, gp = guinea pig)

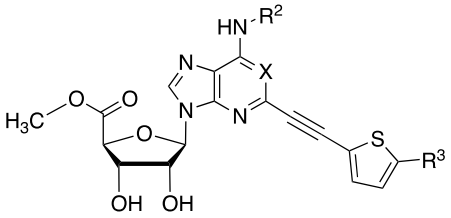

6 – 10

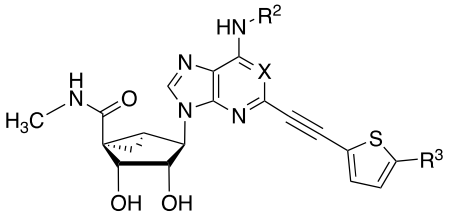

4, **11 – 19**

Compd. (MRS#, PDSP#)	R^2, R^3, X	Off-target binding, K_i, μM (or IC_{50}[f]), or % inhibition[a]
6 MRS7294 42206	Me, Cl, N	DAT -*134%*
7 MRS7295 42207	*n*-Pr, Cl, N	DAT -*41%*
8 MRS7432 49028	Me, F, N	DAT -*234%*, σ_2 1.83
9 MRS7433 49029	*n*-Pr, F, N	DAT -*40%*, σ_1 3.26 (gp), σ_2 0.98
10 MRS7424 48846	Me, F, CH	σ_2 2.22
4 MRS5980	Me, Cl, N	DAT -*556%*, TSPO 0.68±0.18, σ_1 1.40 (gp), σ_2 0.527±0.088
11 MRS7135	Et, Cl, N	DAT -*329%*
12 MRS7154	*n*-Pr, Cl, N	DAT -*159%*, TSPO 1.31±0.21, β_3 1.44
13 MRS7140	Me, Cl, CH	σ_2 3.11 (gp), β_3 1.96
14 MRS7144	Et, Cl, CH	$5HT_{2B}$ 2.21±0.34, TSPO 3.21, β_3 1.44
15 MRS7161 48644	*n*-Pr, Cl, CH	$5HT_{2B}$ 0.76, β_3 1.68, DAT 3.94, TSPO 4.83, σ_2, 1.27

16 MRS7334 44294	Me, F, N	DAT -*144%*, TSPO, 3.38
17 MRS7426 48994	*n*-Pr, F, N	σ_2 1.87, DAT -*212%*
18 MRS7345 44510	Me, F, CH	β_3 1.96
19 MRS7346 44511	Et, F, CH	β_3 3.34
20 MRS7296 42208	5′-ester, See Table 1	$5HT_{2C}$ 3.24±1.05, DAT -*99%*
21[b] MRS7292 42073	5′-ester, See Table 1	KOR 3.13±0.53, DAT -*240%*
22[b] MRS7332 44512	5′-ester, See Table 1	KOR 0.806±0.263 TSPO 4.13±0.33 σ_2 1.66±0.38
23 MRS7333 44293	5′-ester, See Table 1	KOR 2.65±0.37, DAT -*228%*, σ_1 4.04 (gp)

Figure S1. PDSP Off-target screening, representative binding curves (human, unless noted).

Unless noted in the text, no significant interactions (<50% inhibition at 10 μM) for any of the nucleosides were found at the following sites (human unless noted): $5HT_{1A}$, $5HT_{1B}$, $5HT_{1D}$, $5HT_{1E}$, $5HT_{2A}$, $5HT_{2B}$, $5HT_{2C}$, $5HT_3$, $5HT_{5A}$, $5HT_6$, $5HT_7$, α_{1A}, α_{1B}, α_{1D}, α_{2A}, α_{2B}, α_{2C}, β_1, β_2, β_3, BZP rat brain site, D_1, D_2, D_3, D_4, D_5, delta opioid receptor (DOR), $GABA_A$, H_1, H_2, H_3, H_4, M_1, M_2, M_5, mu opioid receptor (MOR), σ_1, σ_2, DAT, NET, SERT. Representative curves are shown.

DAT inhibition by compound **8** (MRS7432, 49028).

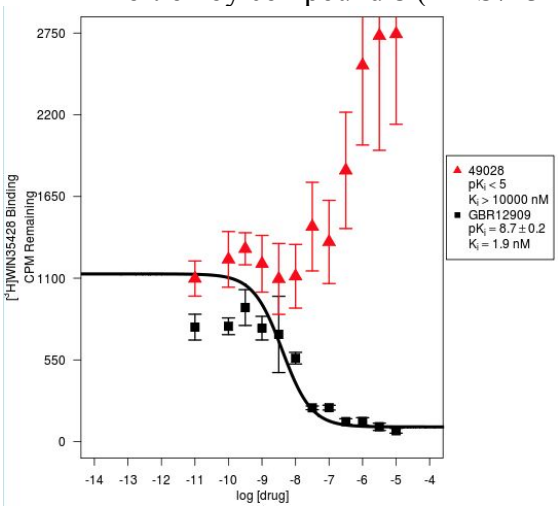

σ_1R (gp) inhibition by compound **9** (MRS7433, 49029).

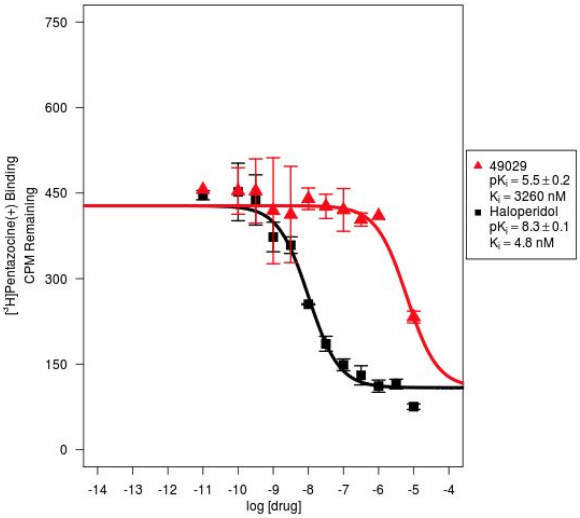

σ_2R inhibition by compound **9** (MRS7433, 49029).

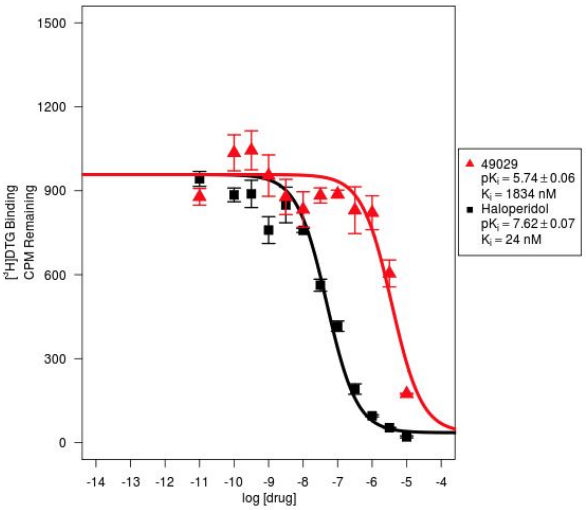

DAT inhibition by compound **15** (MRS7161, 48644).

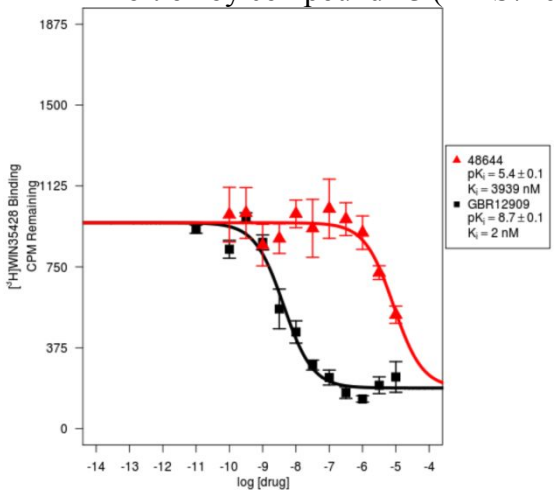

5HT$_{2B}$R inhibition by compound **15** (MRS7161, 48644).

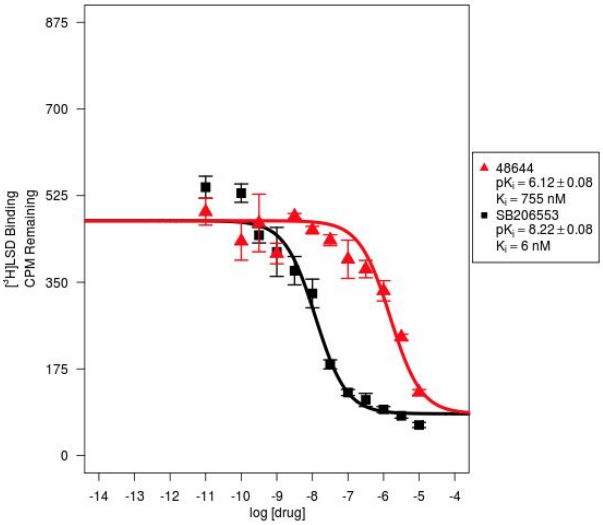

β_3R inhibition by compound **19** (MRS7346, 44511).

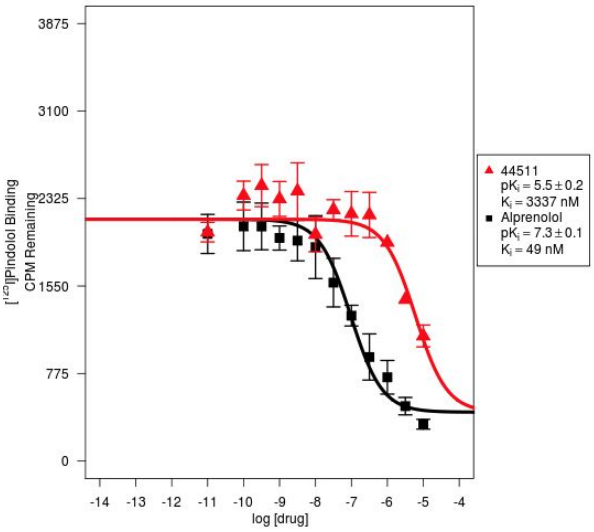
3875
3100
2325
1550
775
0
-14
-13
-12
-11
-10
-9
-8
-7
-6
-5
-4
log [drug]
[125I]Pindolol Binding
CPM Remaining
44511
pKi = 5.5 ± 0.2
Ki = 3337 nM
Alprenolol
pKi = 7.3 ± 0.1
Ki = 49 nM

Figure S2. Rat PK of A_3AR selective nucleosides **4** (A), **11** (B), **14** (C), **16** (D) and **17** (E) (GVK Biosciences, Hyderabad, India.).

A

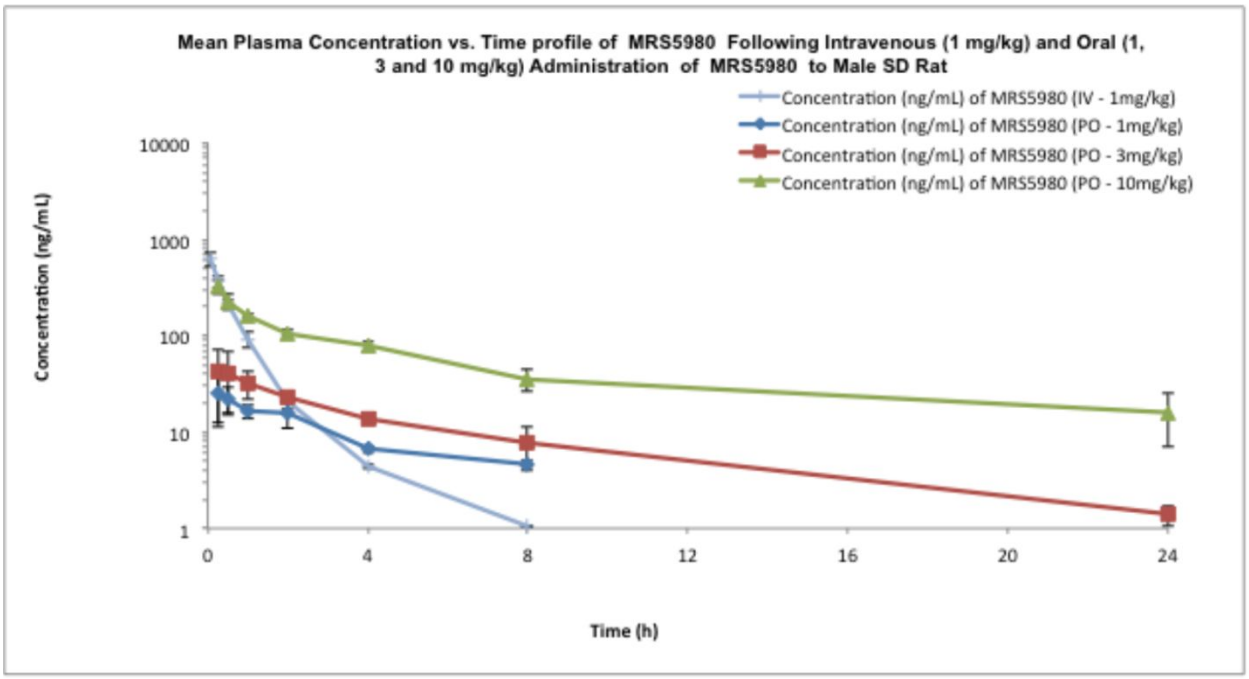

	i.v.	p.o.		
	1 mg/kg	1 mg/kg	3 mg/kg	10 mg/kg
Bioavailability		22 ± 0.3	19 ± 3.5	33 ± 2.2
$t_{1/2}$ (h)	0.7 ± 0.3	3.6 ± 0.4	5.3 ± 0.8	7.8 ± 2.0
C_{max}				
ng/ml		29± 8.6	47 ± 24	326± 57
nM		63 ± 19	101 ± 53	711 ± 125

B

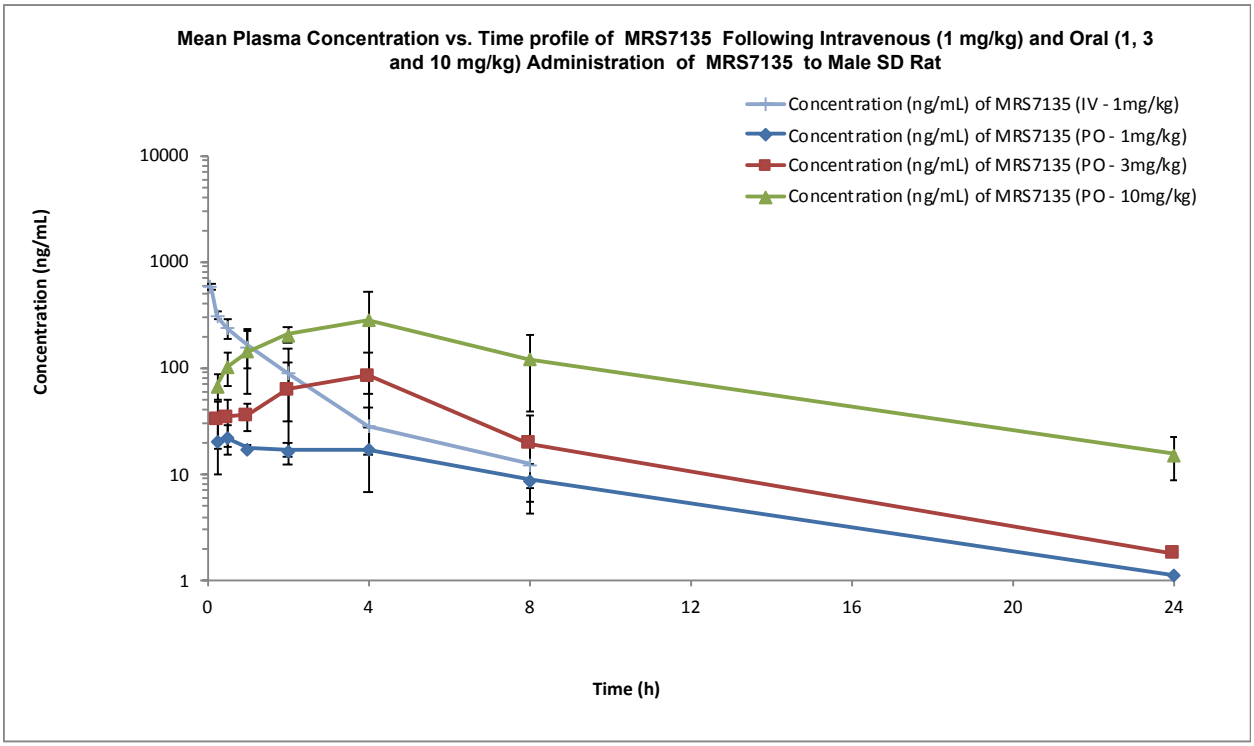

Parameter	1 mg/kg	3 mg/kg	10 mg/kg
$t_{1/2}$ (h), oral adminstration	7.07±1.25	3.31±0.88	5.33±2.13
Bioavailability (%F)	22.3±3.0	26.6±18.1	37.9±13.3

C

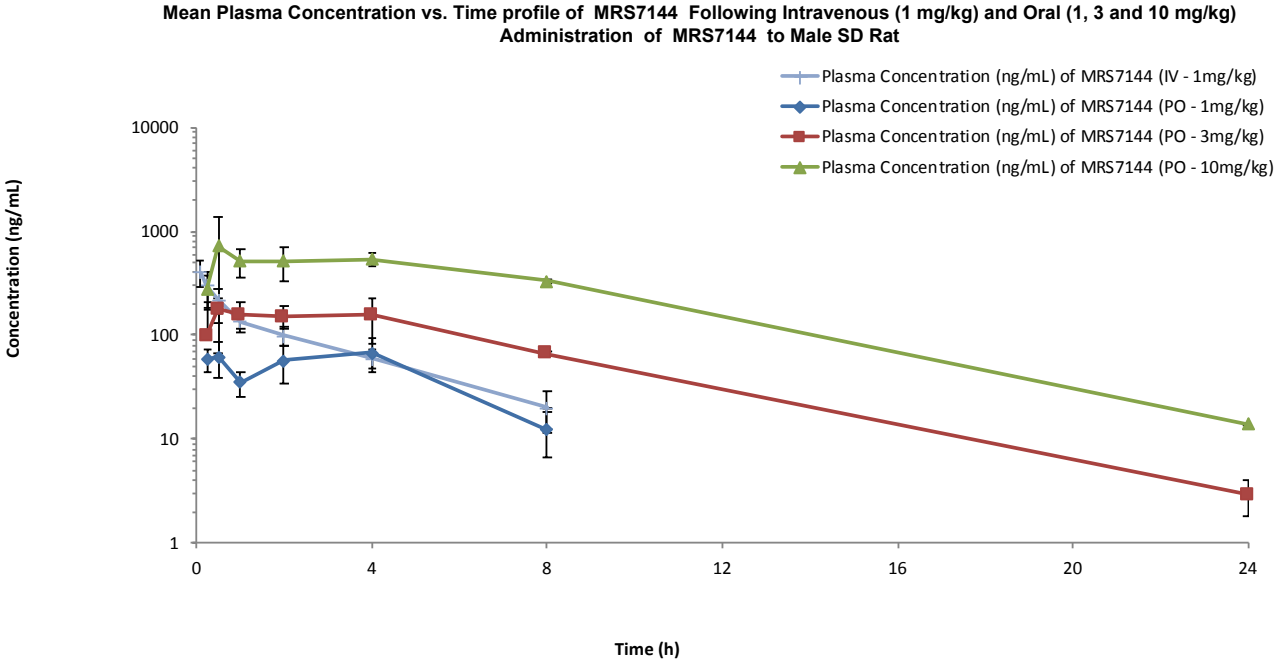

	IV-1 mg/kg	PO-1 mg/kg	PO-3 mg/kg	PO-10 mg/kg
$AUC_{0\text{-last}}$ (ng·h/mL)	711.99	342.56	1331.04	5314.92
$AUC_{0\text{-inf}}$ (ng·h/mL)	745.00	390.47	1345.65	5389.32
Bioavailability	---	52.41	60.21	72.34
$t_{1/2}$ (hr)	2.62±0.90	2.53±0.49	3.50±0.04	3.71±0.14

D

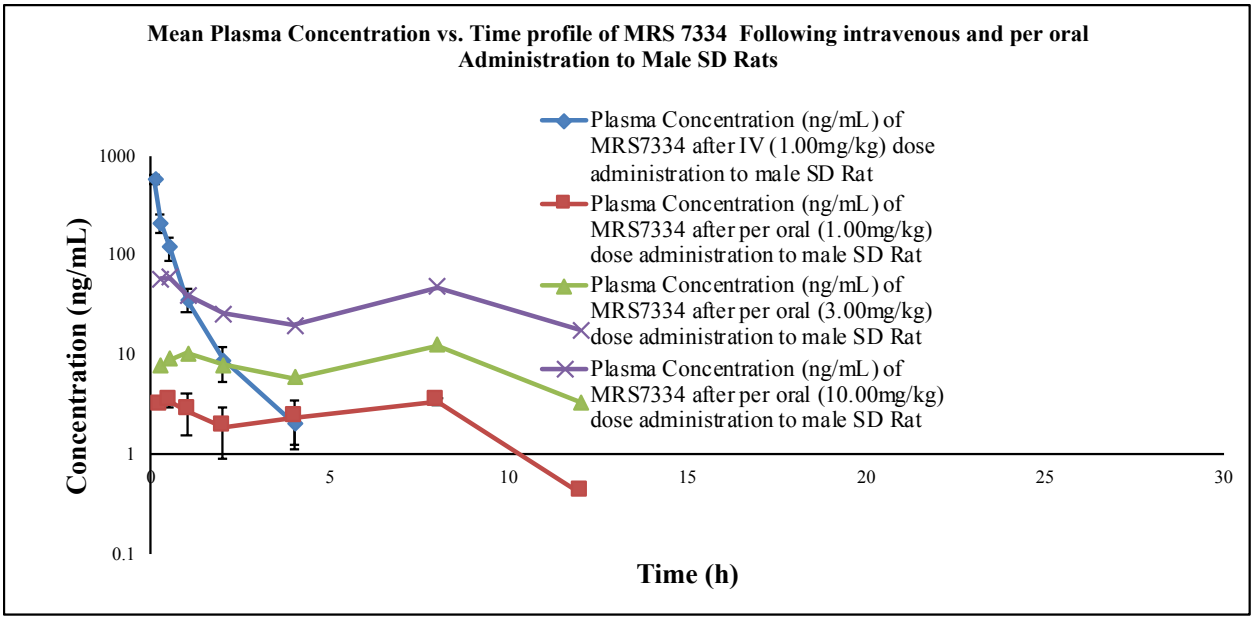

Parameter (MRS7334)	**Mean**	St Dev	%CV
Dose (mg/kg)	**10.00**	0.00	0.00
Cmax (ng/mL)	**66.35**	9.23	13.91
T_{max} (h)	**2.83**	4.47	157.92
$AUC_{0\text{-}last}$ (ng·h/mL)	**400.60**	120.48	30.08
$AUC_{0\text{-}inf}$ (ng·h/mL)	**622.74**	451.15	72.45
AUC_{Extra}(%)	**30.94**	24.69	79.80
$MRT_{0\text{-}last}$ (h)	**5.78**	0.76	13.14
F (%)	**14.48**	0.94	6.51
Rsq	**0.54**	0.24	45.11

E

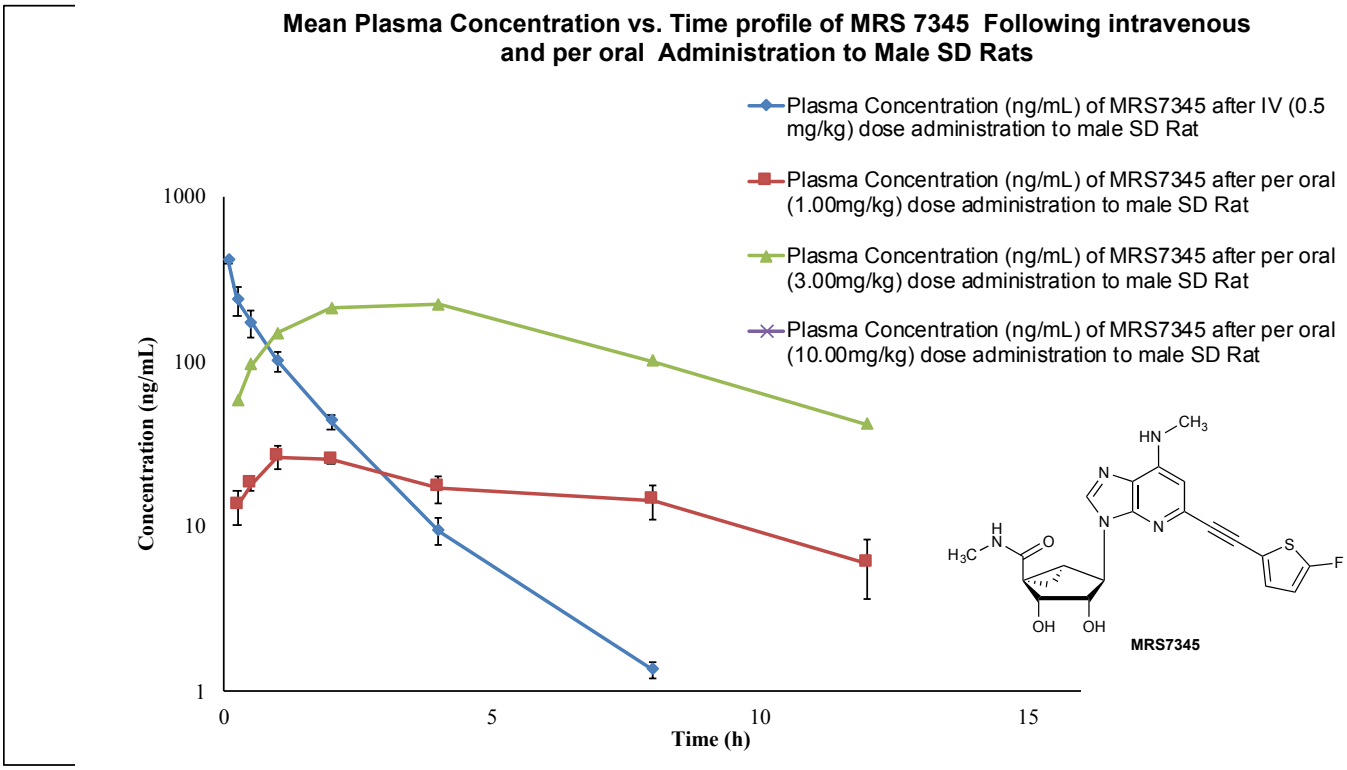

	IV-1 mg/kg	PO-1 mg/kg	PO-3 mg/kg	PO-10 mg/kg
$AUC_{0\text{-last}}$ (ng·h/mL)	503.86	185.8±10.5	1566±608	-
$AUC_{0\text{-inf}}$ (ng·h/mL)	512.53	237.3±43.1	1578±602	-
Bioavailability (%F)	--	28.3±1.1	98.9±37.7	-
t_{max}	-	1.33±0.58	2.67±1.15	-
$t_{1/2}$	1.12±0.10	-	-	

Table S2. In vitro and in vivo ADME-tox data for five representative A_3AR (N)-methanocarba agonists, determined by GVK Biosciences, Hyderbad, India..[a]

Test	**4, MRS5980**[b]	**11, MRS7135**[b]	**14, MRS7144**[b]	**16, MRS7334**	**17, MRS7345**
Simulated gastric fluid (% remaining, min)	100 (120)	92.9 (240)	89.5 (240)	100 (120)	ND
Simulated intestinal fluid (% remaining, min)	100 (120)	91.7 (240)	100 (240)	86.2 (120)	ND
CYP1A2 (IC_{50}, μM)	>10	>10	>10	>30	>30
CYP2C9 (IC_{50}, μM)	>10	>10	>10	>30	>30
CYP2C19 (IC_{50}, μM)	>10	>10	>10	>30	>30
CYP2D6 (IC_{50}, μM)	>10	>10	>10	>30	>30
CYP3A4 (IC_{50}, μM)	>10	>10	>10	>30	>30
Plasma stability, 3 species[d] (% remaining at 120 min)	97.1 (h); 100 (r); 100 (m)	99.0 (h); 93.9 (r); 100 (m)	86.4 (h); 93.2 (r); 100 (m)	100 (h); 100 (r); 97.3 (m)	98.1 (h); 81.5 (r); 96.0 (m)
Plasma protein binding, 3 species[d] (%)	93.8 (h); 94.1 (r); 93.6 (m)	97.0 (h); 93.9 (r); 96.8 (m)	99.64 (h); 99.22 (r); 99.5 (m)	ND	ND
CACO2 permeability (P_{app}, A to B (10^{-6} cm/sec); efflux ratio)	2.20; 16.2	0.80; 40.1	2.05; 6.40	0.87; 53.1	4.89; 9.57
Liver microsomal stability, 3 species[d] ($t_{1/2}$, min)	230 (h), 128 (r), 143 (m)	203 (h), 155 (r), 95.4 (m)	145 (h), 104 (r), 98.6 (m)	141 (h), 145 (r), 117 (m)	60.6 (h), 41.9 (r), 117 (m)
HEP G2 cell toxicity, CC_{50} (μM)	>100	>30	ND	>30	ND
aqueous solubility[c] (pH 7.4, unless noted, μg/mL)	16.8±1.1; 19.7±0.5 (pH 4.0)	4.22	5.37±0.48	ND	167±5

[a] Procedure is in the Supporting Information of Tosh et al., *J. Med. Chem.*, 2014, 57: 9901-9914.
[b] Compounds previously reported in Tosh et al.: 1) *J. Med. Chem.*, 2014, 57: 9901-9914; 2) *ACS Med. Chem. Lett.*, 2015, 6:804-808.
[c] Mean ± SD, pION method.
[d] Species tested were human, rat and mouse; species as indicated.

Molecular Modeling

Ligand-Protein Complex Preparation

A homology model of hA_3AR was retrieved from a previous work, where it was built with the Prime knowledge-based method[1,2], using as templates a structure of $hA_{2A}AR$ (3QAK[3], plus 4UHR[4] to model IL3) for the greater part of the receptor and a structure of hA_1AR (5UEN[5]) for TM2. The Protein Preparation Wizard tool[6] of the Schrödinger suite (Maestro 2019-1)[7] was used to assign the histidines protonation and tautomeric states, with His79, His95, His124 and His158 protonated at N^{ε} nitrogen (named HSE according to the CHARMM nomenclature), while His272 protonated at N^{δ} (HSD). The Ballesteros-Weinstein[8] numbering was used throughout the manuscript to define the residues of the receptor.

Ligands were drawn using the Schrödinger suite (Maestro 2019-1)[7] and minimized using the OPLS3 force field.[9]

Molecular Docking

Compounds **16** and **8** were docked to the hA_3AR homology model with Glide-XP[10] scoring function, on a grid of 30 Å side, centered on Asn250 (Asn6.55) and Phe168 (EL2). Successively, a pose was selected for each compound by visual inspection.

Molecular Dynamics

The systems obtained from docking were prepared for MD simulations employing the HTMD[11] module, adding to the system a water molecule mediating the interaction among Asn250 (Asn6.55), Ser247 (Ser6.52) and Met177 (Met5.38), as previously reported.[12] Each protein-ligand complex was oriented using the Positioning of Proteins in Membrane (PPM)[13] web server and inserted into a 90 Å x 90 Å 1-palmitoyl-2-oleoyl-sn-glycero-3-phosphocholine (POPC) lipid bilayer generated with the VMD Membrane Plugin.[14] Each system was solvated with TIP3P[15] water molecules (with a positive and negative padding of 15 Å on the *z* axis) and neutralized with Na^+/Cl^- counter-ions, added to reach a concentration of 0.154 M.

The compounds were also simulated in the free (unbound) state: they were inserted at the center of a 40 Å sided water box and simulated in the conditions discussed below.

The simulations were carried out employing CHARMM36[16,17] force field for protein, lipids, water and ions, CGenFF[18,19] force field for the ligand, and ACEMD[20] as molecular dynamics engine.

Missing ligand parameters were assigned by analogy using the ParamChem[21] web service, with few modifications on the (N)-methanocarba parameters, assigned manually according to the carbocyclic parameters present in the CGenFF.

The initial system was minimized through 5000 conjugate-gradient steps and equilibrated for 40 ns MD simulation in the NPT ensemble, where positional harmonic restraints were applied to ligand and protein atoms (0.8 kcal mol^{-1} $Å^{-2}$ for ligand atoms, 0.85 kcal mol^{-1} $Å^{-2}$ for Cα carbon atoms, and 0.4 kcal mol^{-1} $Å^{-2}$ for the other protein atoms) and linearly reduced in the last 20 ns. After equilibration, three 30 ns replicates of MD simulations were run for each system in the NVT ensemble. The pressure was maintained at around 1 atm by a Berendsen barostat (relaxation time 800 fs) during equilibration and temperature was kept at around 310 K by a Langevin thermostat (damping constant 1 ps^{-1} and 0.1 ps^{-1} for equilibration and production, respectively). The timestep was set to 2 fs in all the simulations and the M-SHAKE[22] algorithm was used to constrain bonds containing hydrogen atoms. A 9 Å cutoff was employed for non-bonded interactions, with a switching distance of 7.5 Å, and the long-range electrostatic interactions beyond the cutoff were computed with the Particle Mesh Ewald (PME)[23] method (1Å grid spacing).

Trajectory Analysis

An in-house Tcl script employing VMD 1.9.3 was used to analyze the MD trajectories.[14] The systems were aligned to their initial conformation by superposing protein Cα carbon atoms. Ligand-protein electrostatic and van der Waals interactions were computed with NAMD.[24] The data were plotted using the Gnuplot (version 5.0) software.[25]

The puckering parameters (phase angle of pseudorotation (*P*) and degree of deformation from the plane (ν_{max})) were computed with an in-house python2.7 script, employing the ProDy[26] and matplotlib[27] modules.

References:

1. Jacobson, M. P.; Pincus, D. L.; Rapp, C. S.; Day, T. J. F.; Honig, B.; Shaw, D. E.; Friesner, R. A. A Hierarchical Approach to All-Atom Protein Loop Prediction. *Proteins* **2004**, *55* (2), 351–367.
2. Jacobson, M. P.; Friesner, R. A.; Xiang, Z.; Honig, B. On the Role of the Crystal Environment in Determining Protein Side-Chain Conformations. *J. Mol. Biol.* **2002**, *320* (3), 597–608.
3. Xu, F.; Wu, H.; Katritch, V.; Han, G. W.; Jacobson, K. A.; Gao, Z.-G.; Cherezov, V.; Stevens, R. C. Structure of an Agonist-Bound Human A2A Adenosine Receptor. *Science* **2011**, *332* (6027), 322–327.
4. Lebon, G.; Edwards, P. C.; Leslie, A. G. W.; Tate, C. G. Molecular Determinants of CGS21680 Binding to the Human Adenosine A2A Receptor. *Mol. Pharmacol.* **2015**, *87* (6), 907–915.
5. Glukhova, A.; Thal, D. M.; Nguyen, A. T.; Vecchio, E. A.; Jörg, M.; Scammells, P. J.; May, L. T.; Sexton, P. M.; Christopoulos, A. Structure of the Adenosine A1 Receptor Reveals the Basis for Subtype Selectivity. *Cell* **2017**, *168* (5), 867-877.e13.
6. Sastry, G. M.; Adzhigirey, M.; Day, T.; Annabhimoju, R.; Sherman, W. Protein and Ligand Preparation: Parameters, Protocols, and Influence on Virtual Screening Enrichments. *J. Comput. Aided Mol. Des.* **2013**, *27* (3), 221–234.
7. Schrödinger Release 2019-3: Maestro, Schrödinger, LLC, New York, NY, 2019.
8. Ballesteros, J. A.; Weinstein, H. [19] Integrated Methods for the Construction of Three-Dimensional Models and Computational Probing of Structure-Function Relations in G Protein-Coupled Receptors. In *Receptor Molecular Biology*; Methods in Neurosciences; Elsevier, 1995; Vol. 25, pp 366–428.
9. Harder, E.; Damm, W.; Maple, J.; Wu, C.; Reboul, M.; Xiang, J. Y.; Wang, L.; Lupyan, D.; Dahlgren, M. K.; Knight, J. L.; et al. OPLS3: A Force Field Providing Broad Coverage of Drug-like Small Molecules and Proteins. *J. Chem. Theory Comput.* **2016**, *12* (1), 281–296.
10. Friesner, R. A.; Murphy, R. B.; Repasky, M. P.; Frye, L. L.; Greenwood, J. R.; Halgren, T. A.; Sanschagrin, P. C.; Mainz, D. T. Extra Precision Glide: Docking and Scoring Incorporating a Model of Hydrophobic Enclosure for Protein-Ligand Complexes. *J. Med. Chem.* **2006**, *49* (21), 6177–6196.
12. Tosh, D. K.; Salmaso, V.; Rao, H.; Bitant, A.; Fisher, C. L.; Lieberman, D. I.; Vorbrüggen, H.; Reitman, M. L.; Gavrilova, O.; Gao, Z. G.; Auchampach, J. A.; Jacobson, K. A. Truncated (N)-methanocarba nucleosides as partial agonists at mouse and human A_3 adenosine receptors: Affinity enhancement by N^6-(2-phenylethyl) substitution. J. Med. Chem., ACS Spring 2020 National Meeting & Exposition, Philadelphia, PA, Abstr. MEDI150.

11. Doerr, S.; Harvey, M. J.; Noé, F.; De Fabritiis, G. HTMD: High-Throughput Molecular Dynamics for Molecular Discovery. *J. Chem. Theory Comput.* **2016**, *12* (4), 1845–1852.
13. Lomize, M. A.; Pogozheva, I. D.; Joo, H.; Mosberg, H. I.; Lomize, A. L. OPM Database and PPM Web Server: Resources for Positioning of Proteins in Membranes. *Nucleic Acids Res.* **2012**, *40* (Database issue), D370-6.
14. Humphrey, W.; Dalke, A.; Schulten, K. VMD: Visual Molecular Dynamics. *J. Mol. Graph.* **1996**, *14* (1), 33–38, 27.
15. Jorgensen, W. L.; Chandrasekhar, J.; Madura, J. D.; Impey, R. W.; Klein, M. L. Comparison of Simple Potential Functions for Simulating Liquid Water. *J. Chem. Phys.* **1983**, *79* (2), 926.
16. Best, R. B.; Zhu, X.; Shim, J.; Lopes, P. E. M.; Mittal, J.; Feig, M.; Mackerell, A. D. Optimization of the Additive CHARMM All-Atom Protein Force Field Targeting Improved Sampling of the Backbone φ, ψ and Side-Chain χ(1) and χ(2) Dihedral Angles. *J. Chem. Theory Comput.* **2012**, *8* (9), 3257–3273.
17. Klauda, J. B.; Venable, R. M.; Freites, J. A.; O'Connor, J. W.; Tobias, D. J.; Mondragon-Ramirez, C.; Vorobyov, I.; MacKerell, A. D.; Pastor, R. W. Update of the CHARMM All-Atom Additive Force Field for Lipids: Validation on Six Lipid Types. *J. Phys. Chem. B* **2010**, *114* (23), 7830–7843.
18. Vanommeslaeghe, K.; MacKerell, A. D. Automation of the CHARMM General Force Field (CGenFF) I: Bond Perception and Atom Typing. *J. Chem. Inf. Model.* **2012**, *52* (12), 3144–3154.
19. Vanommeslaeghe, K.; Raman, E. P.; MacKerell, A. D. Automation of the CHARMM General Force Field (CGenFF) II: Assignment of Bonded Parameters and Partial Atomic Charges. *J. Chem. Inf. Model.* **2012**, *52* (12), 3155–3168.
20. Harvey, M. J.; Giupponi, G.; Fabritiis, G. D. ACEMD: Accelerating Biomolecular Dynamics in the Microsecond Time Scale. *J. Chem. Theory Comput.* **2009**, *5* (6), 1632–1639.
21. CHARMM General Force Field (CGenFF) program, https://cgenff.umaryland.edu/
22. Kräutler, V.; van Gunsteren, W. F.; Hünenberger, P. H. A Fast SHAKE Algorithm to Solve Distance Constraint Equations for Small Molecules in Molecular Dynamics Simulations. *J. Comput. Chem.* **2001**, *22* (5), 501–508.
23. Essmann, U.; Perera, L.; Berkowitz, M. L.; Darden, T.; Lee, H.; Pedersen, L. G. A Smooth Particle Mesh Ewald Method. *J. Chem. Phys.* **1995**, *103* (19), 8577.
24. Phillips, J. C.; Braun, R.; Wang, W.; Gumbart, J.; Tajkhorshid, E.; Villa, E.; Chipot, C.; Skeel, R. D.; Kalé, L.; Schulten, K. Scalable Molecular Dynamics with NAMD. *J. Comput. Chem.* **2005**, *26* (16), 1781–1802.
25. Williams, T.; Kelley, C. Gnuplot 5.0, http://www.gnuplot.info
26. Bakan, A.; Meireles, L. M.; Bahar, I. ProDy: Protein Dynamics Inferred from Theory and Experiments. *Bioinformatics* **2011**, *27* (11), 1575–1577.
27. Hunter, J. D. Matplotlib: A 2D Graphics Environment. *Comput. Sci. Eng.* **2007**, *9* (3), 90–95.

Table S3

Compound		**Cmp 8 (MRS7432)**			**Cmp 16 (MRS7334)**		
Replicates		**1**	**2**	**3**	**1**	**2**	**3**
$RMSD_{ave}$ (Å)		1.85	1.60	1.84	2.03	1.84	2.21
En_{ave} (kcal/mol)	**Ele**	-25.85	-26.10	-25.30	-29.51	-22.39	-25.38
	vdW	-38.33	-39.05	-38.70	-46.54	-42.46	-42.75
	Total	-64.18	-65.15	-64.00	-76.05	-64.85	-68.13
Hydrogen Bonds	**Thr94 3.36**	88%	82%	86%	69%	69%	43%
	Asn250 6.55	93%	96%	86%	88%	89%	89%
	Ser271 7.42	23%	38%	14%	1%	10%	5%
	His272 7.43	3%	6%	4%	84%	0%	50%

Table S3. Summary of the MD trajectories analysis of the complexes between hA_3 AR and compounds **8** and **16**. The following average values are reported: the average root mean square deviation of the ligand heavy atoms relative to the docking pose ($RMSD_{ave}$), after alignment of the protein Cα atoms to the starting structure; the average ligand-receptor electrostatic (Ele), van der Waals (vdW) and sum of the two (Total) interaction energy (En_{ave}). The percentages of frames showing hydrogen bonds between the ligand and Thr94 (3.36), Asn250 (6.55), Ser271 (7.42) and His272 (7.43) are indicated. The replicates discussed in the manuscript (selected on the basis of the lowest average total interaction energy) are highlighted in red.

Figure S3

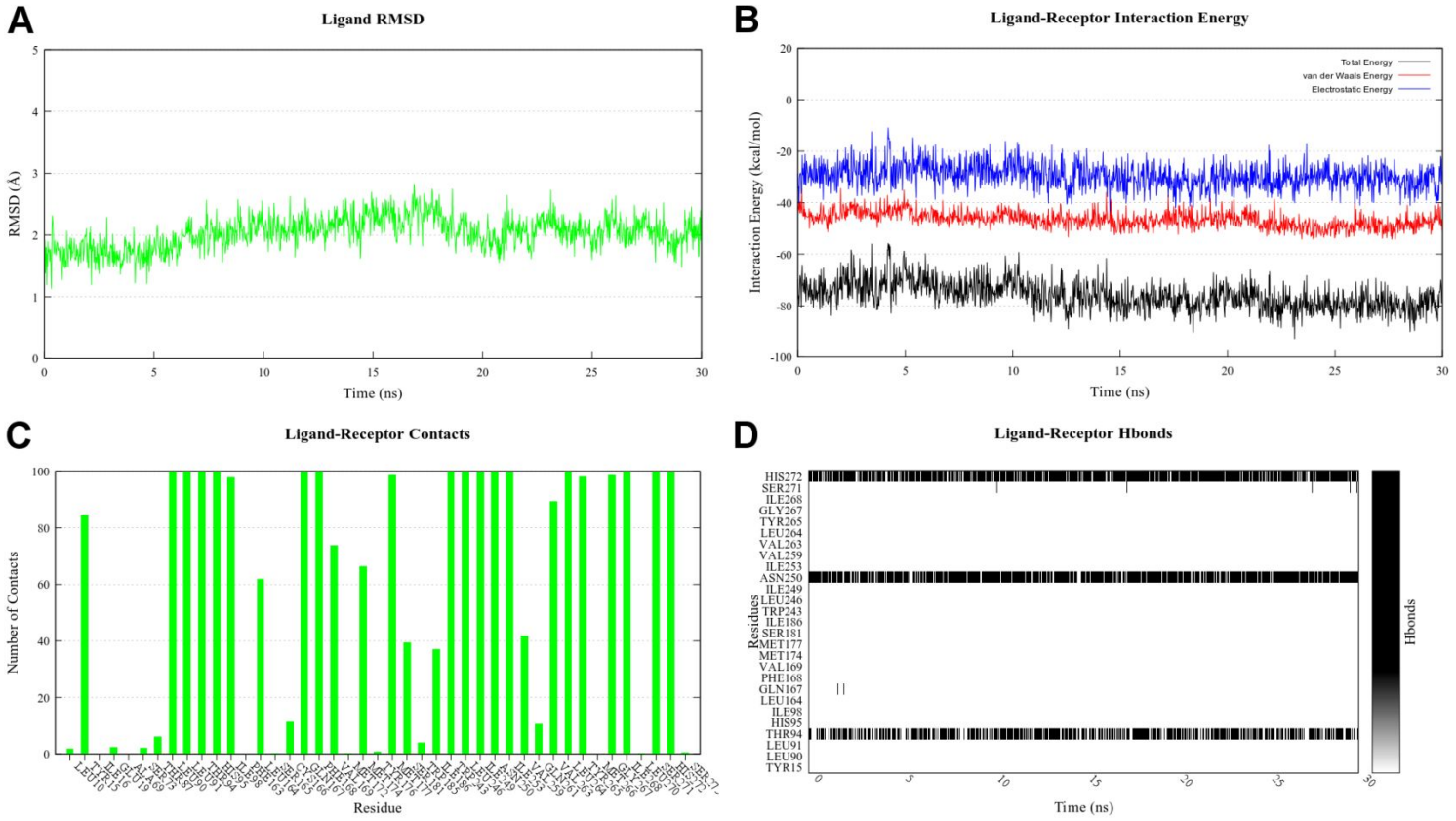

Figure S3. Analysis of the MD simulation (replicate 1) of the complex between compound **16** and hA_3AR. The replicate was chosen on the basis of the lowest average total interaction energy. **A)** RMSD of ligand heavy atoms relative to the docking pose, after alignment of the protein Cα atoms to the starting structure. **B)** Electrostatic and van der Waals (and Total, as sum of the two) ligand-receptor interaction energy. **C)** Histograms showing the percentage of time where each protein residue is in contact (distance < 4 Å) with the ligand. Residues with 0 contacts during the simulations are not reported. **D)** Presence of hydrogen bonds during the simulation for selected residues (residues that are in contact with the ligand at least for one third of the simulation).

Figure S4

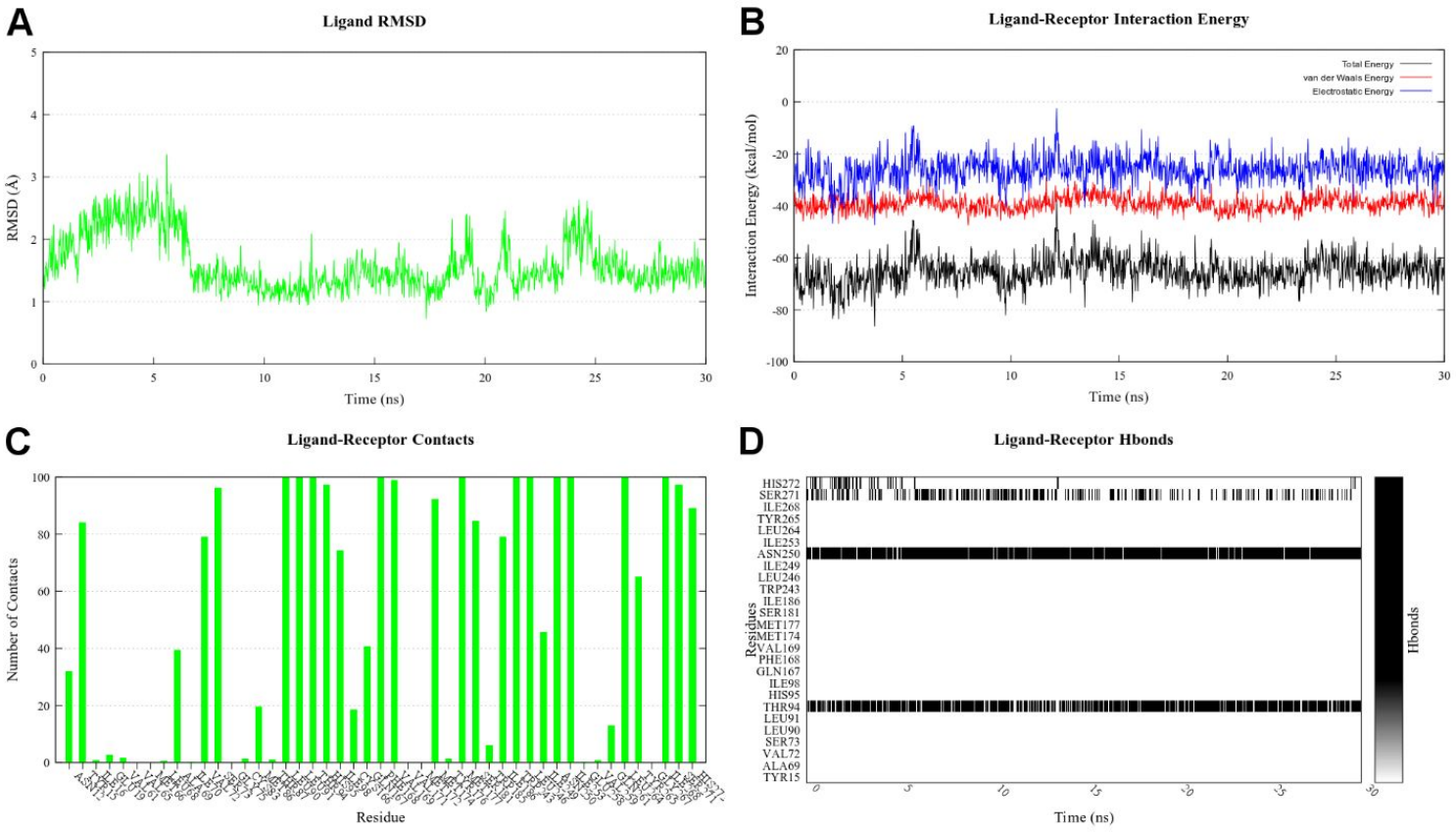

Figure S4. Analysis of the MD simulation (replicate 2) of the complex between compound **8** and hA_3AR. The replicate was chosen on the basis of the lowest average total interaction energy. **A)** RMSD of ligand heavy atoms relative to the docking pose, after alignment of the protein Cα atoms to the starting structure. **B)** Electrostatic and van der Waals (and Total, as sum of the two) ligand-receptor interaction energy. **C)** Histograms showing the percentage of time where each protein residue is in contact (distance < 4 Å) with the ligand. Residues with 0 contacts during the simulations are not reported. **D)** Presence of hydrogen bonds during the simulation for selected residues (residues that are in contact with the ligand at least for one third of the simulation).

Figure S5

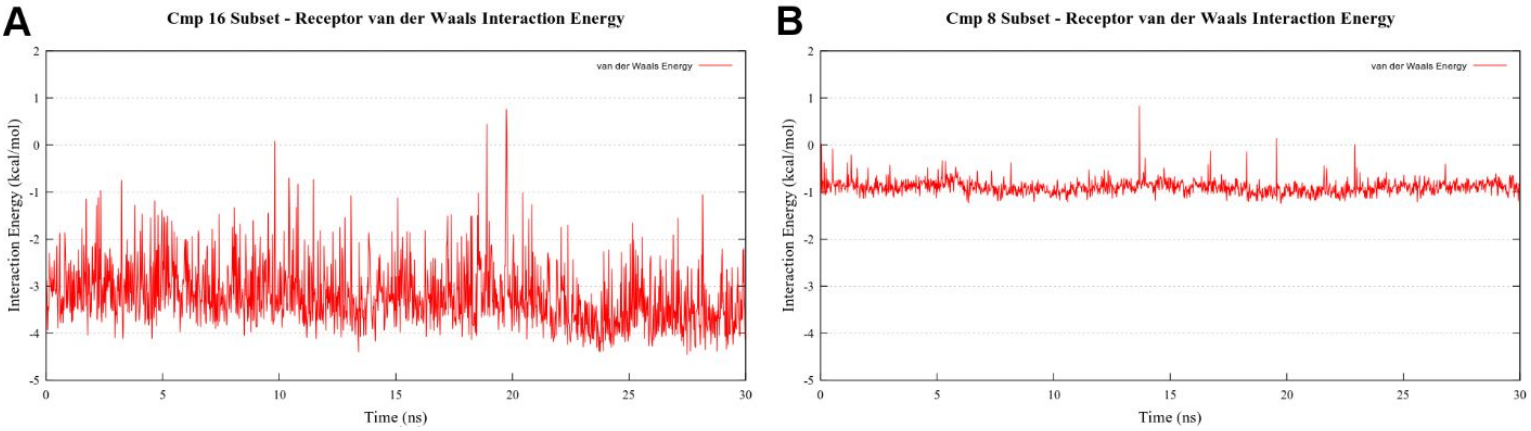

Figure S5. van der Waals interaction energy during the MD simulation between **A)** the receptor and the carbon and hydrogen atoms replacing O4' in compound **16**; **B)** the receptor and O4' of compound **8**.

Figure S6

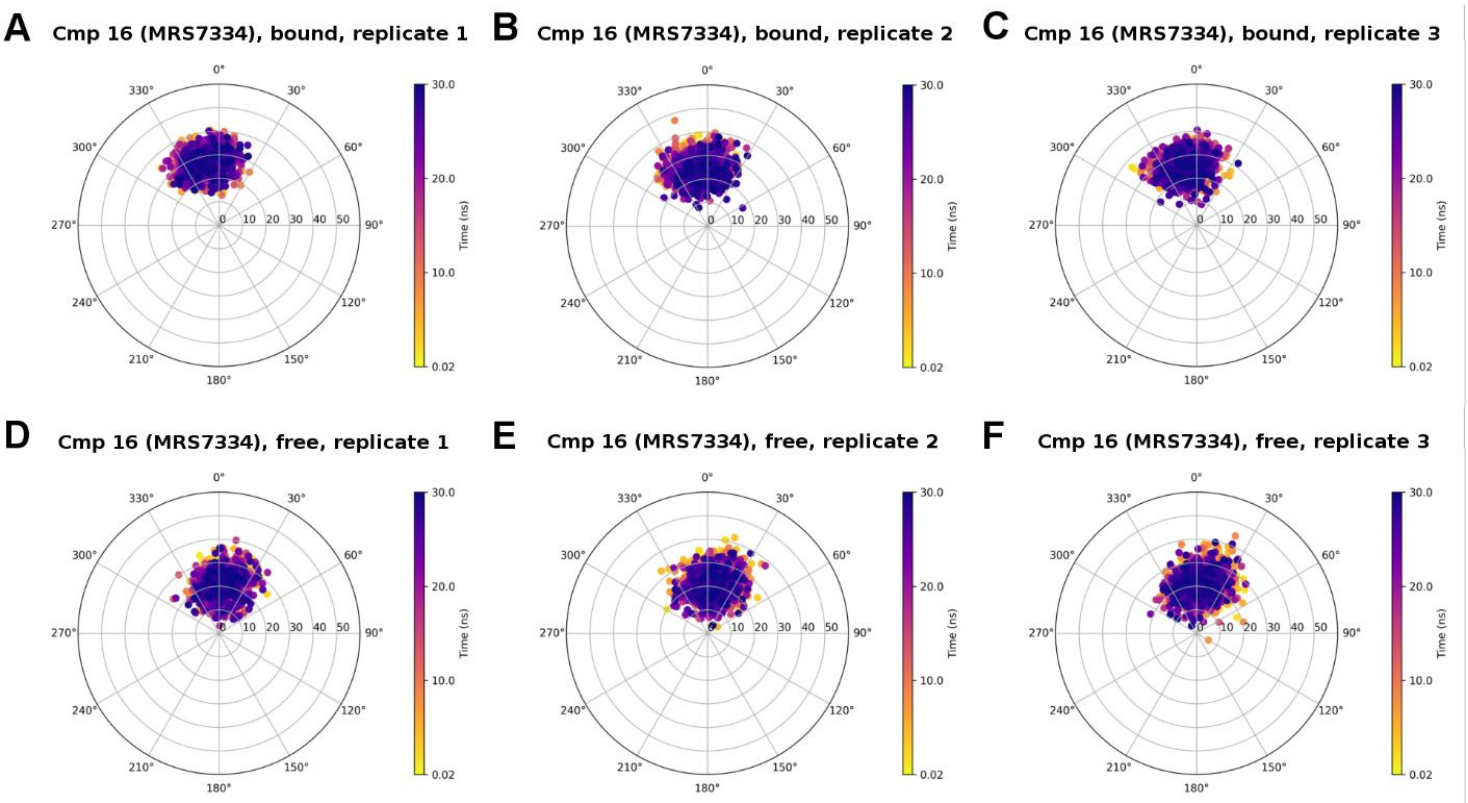

Figure S6. Conformation of the (N)-methanocarba moiety of compound **16** expressed as phase angle of pseudorotation (*P*) and degree of deformation from the plane (ν_{max}), reported respectively on the polar axis and on the *x*/*y* axes of the pseudorotational cycle. The time-coordinate is

represented by a colorimetric scale going from yellow to dark purple. Plots **A-B-C**) represent the puckering of the (N)-methanocarba when the compound is bound to the receptor, in replicates 1, 2 and 3, respectively. Plots **D-E-F**) represent the puckering of the (N)-methanocarba when the compound is simulated in an un-bound state, in solution, in three different replicates.

Figure S7

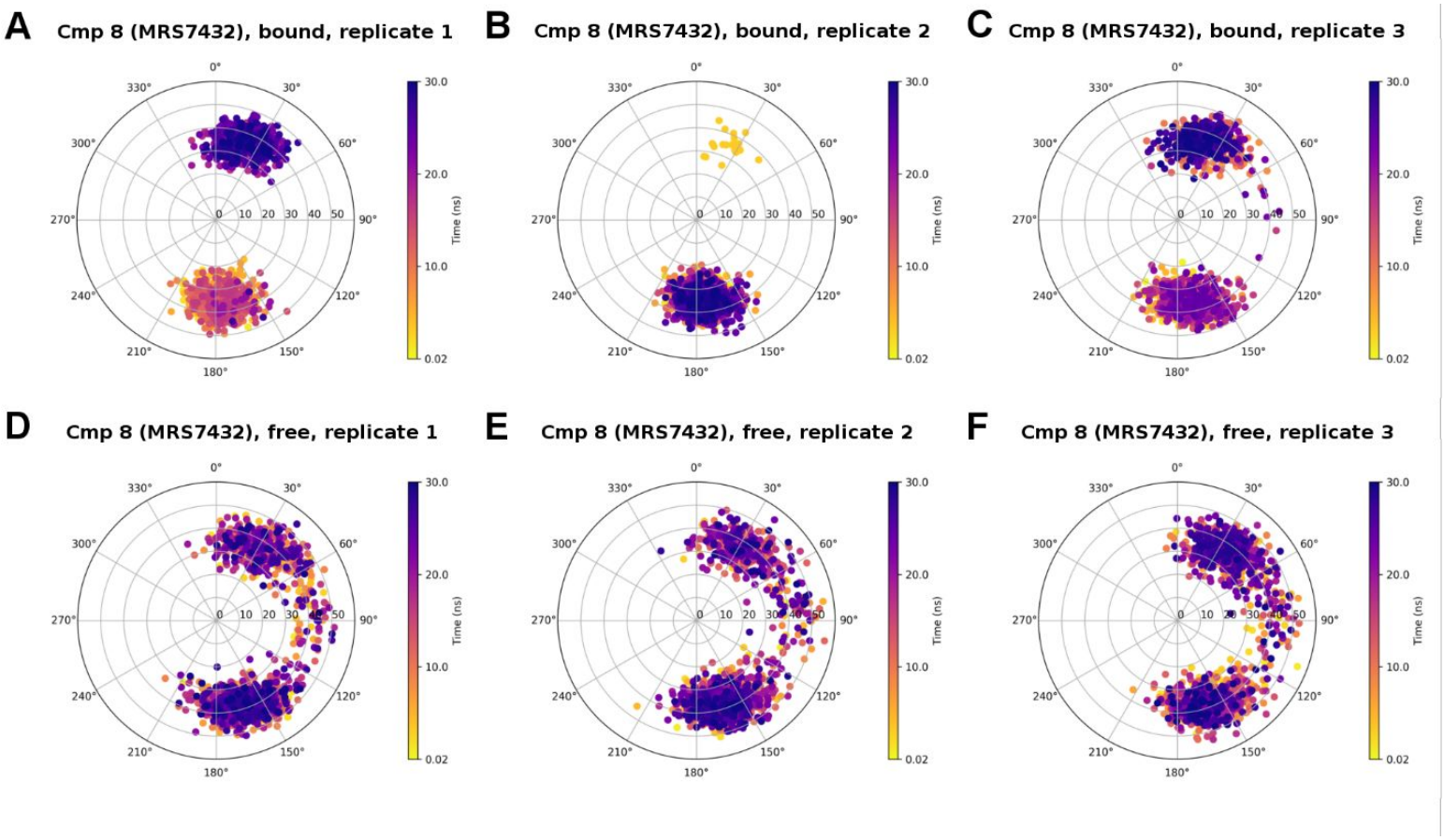

Figure S7. Conformation of the ribose-like ring of compound **8** expressed as phase angle of pseudorotation (*P*) and degree of deformation from the plane (ν_{max}), reported respectively on the polar axis and on the *x*/*y* axes of the pseudorotational cycle. The time-coordinate is represented by a colorimetric scale going from yellow to dark purple. Plots **A-B-C**) represent the puckering of ribose-like ring when the compound is bound to the receptor, in replicates 1, 2 and 3, respectively. Plots **D-E-F**) represent the puckering of the ribose-like ring when the compound is simulated in an un-bound state, in solution, in three different replicates.

Video S1. MD trajectory (replicate 1) of the complex between compound **16** (**MRS7334**) and hA_3AR, after superposition of receptor Cα atoms to the initial frame. The receptor is depicted by a grey ribbon and the ligand by green sticks. The transparency of TM7 tip was increased to enable the visualization of the ligand. Key receptor residues are highlighted by sticks. Hydrogen bonds are shown by dashed lines.

Video S2. MD trajectory (replicate 2) of the complex between compound **8** (**MRS7432**) and hA_3AR, after superposition of receptor Cα atoms to the initial frame. The receptor is depicted by a grey ribbon and the ligand by orange sticks. The transparency of TM7 tip was increased to enable the visualization of the ligand. Key receptor residues are highlighted by sticks. Hydrogen bonds are shown by dashed lines.

Table S4. Screening of compound **4** (MRS5980) by DiscoverX (Eurofins DiscoverX Corporation, Fremont, CA 94538 USA) broadly at G protein-coupled receptors (GPCRs) and at kinases.

A. Compound **4** (10 µM) tested as agonist in GPCRMax screen (167 known GPCRs). ADORA3 (A_3AR) is the only hit.

GPCR ID	Customer	Compound ID	Assay Mode	Conc [µM]	Mean RLU	% Activity
ADCYAP1R1	NIH	MRS5980	Agonist	10	222880	0%
ADORA3	NIH	MRS5980	Agonist	10	592620	168%
ADRA1B	NIH	MRS5980	Agonist	10	210280	0%
ADRA2A	NIH	MRS5980	Agonist	10	441000	0%
ADRA2B	NIH	MRS5980	Agonist	10	268660	4%
ADRA2C	NIH	MRS5980	Agonist	10	133560	-1%
ADRB1	NIH	MRS5980	Agonist	10	211260	1%
ADRB2	NIH	MRS5980	Agonist	10	49840	0%
AGTR1	NIH	MRS5980	Agonist	10	496720	-3%
AGTRL1	NIH	MRS5980	Agonist	10	401660	0%
AVPR1A	NIH	MRS5980	Agonist	10	22260	0%
AVPR1B	NIH	MRS5980	Agonist	10	35140	0%
AVPR2	NIH	MRS5980	Agonist	10	796320	1%
BDKRB1	NIH	MRS5980	Agonist	10	25480	0%
BDKRB2	NIH	MRS5980	Agonist	10	530740	-2%
BRS3	NIH	MRS5980	Agonist	10	364280	4%
C3AR1	NIH	MRS5980	Agonist	10	41020	0%
C5AR1	NIH	MRS5980	Agonist	10	136080	1%
C5L2	NIH	MRS5980	Agonist	10	447020	3%
CALCR	NIH	MRS5980	Agonist	10	33040	0%
CALCRL-RAMP1	NIH	MRS5980	Agonist	10	85680	0%
CALCRL-RAMP2	NIH	MRS5980	Agonist	10	209720	4%
CALCRL-RAMP3	NIH	MRS5980	Agonist	10	450240	2%
CALCR-RAMP2	NIH	MRS5980	Agonist	10	167020	8%
CALCR-RAMP3	NIH	MRS5980	Agonist	10	14000	-1%
CCKAR	NIH	MRS5980	Agonist	10	43260	0%
CCKBR	NIH	MRS5980	Agonist	10	935060	3%
CCR10	NIH	MRS5980	Agonist	10	97580	1%
CCR1	NIH	MRS5980	Agonist	10	736960	10%
CCR2	NIH	MRS5980	Agonist	10	150640	2%
CCR3	NIH	MRS5980	Agonist	10	123620	7%
CCR4	NIH	MRS5980	Agonist	10	287280	6%
CCR5	NIH	MRS5980	Agonist	10	207760	5%
CCR6	NIH	MRS5980	Agonist	10	196280	3%
CCR7	NIH	MRS5980	Agonist	10	1327620	11%
CCR8	NIH	MRS5980	Agonist	10	35140	0%
CCR9	NIH	MRS5980	Agonist	10	121800	0%
CHRM1	NIH	MRS5980	Agonist	10	846160	2%
CHRM2	NIH	MRS5980	Agonist	10	63560	0%
CHRM3	NIH	MRS5980	Agonist	10	69860	0%
CHRM4	NIH	MRS5980	Agonist	10	586040	-1%
CHRM5	NIH	MRS5980	Agonist	10	552440	-2%
CMKLR1	NIH	MRS5980	Agonist	10	89460	1%
CNR1	NIH	MRS5980	Agonist	10	26320	1%
CNR2	NIH	MRS5980	Agonist	10	153260	-15%
CRHR1	NIH	MRS5980	Agonist	10	291900	1%
CRHR2	NIH	MRS5980	Agonist	10	120960	0%
CRTH2	NIH	MRS5980	Agonist	10	151060	-2%
CX3CR1	NIH	MRS5980	Agonist	10	366800	1%
CXCR1	NIH	MRS5980	Agonist	10	250460	1%
CXCR2	NIH	MRS5980	Agonist	10	220500	4%
CXCR3	NIH	MRS5980	Agonist	10	424900	1%
CXCR4	NIH	MRS5980	Agonist	10	82880	12%
CXCR5	NIH	MRS5980	Agonist	10	263300	1%
CXCR6	NIH	MRS5980	Agonist	10	29260	3%
CXCR7	NIH	MRS5980	Agonist	10	324660	2%
DRD1	NIH	MRS5980	Agonist	10	110740	1%
DRD2L	NIH	MRS5980	Agonist	10	98140	4%
DRD2S	NIH	MRS5980	Agonist	10	233380	3%
DRD3	NIH	MRS5980	Agonist	10	581000	12%
DRD4	NIH	MRS5980	Agonist	10	12880	3%
DRD5	NIH	MRS5980	Agonist	10	31360	2%
EBI2	NIH	MRS5980	Agonist	10	145180	-2%
EDG1	NIH	MRS5980	Agonist	10	174720	-1%
EDG3	NIH	MRS5980	Agonist	10	1139460	12%
EDG4	NIH	MRS5980	Agonist	10	146020	1%
EDG5	NIH	MRS5980	Agonist	10	253260	2%
EDG6	NIH	MRS5980	Agonist	10	423640	-9%
EDG7	NIH	MRS5980	Agonist	10	87780	0%
EDNRA	NIH	MRS5980	Agonist	10	25340	0%
EDNRB	NIH	MRS5980	Agonist	10	98280	2%
F2R	NIH	MRS5980	Agonist	10	153020	1%
F2RL1	NIH	MRS5980	Agonist	10	495040	2%
F2RL3	NIH	MRS5980	Agonist	10	1126720	15%
FFAR1	NIH	MRS5980	Agonist	10	211120	2%
FPR1	NIH	MRS5980	Agonist	10	1310960	12%
FPRL1	NIH	MRS5980	Agonist	10	98140	1%
FSHR	NIH	MRS5980	Agonist	10	211120	-5%
GALR1	NIH	MRS5980	Agonist	10	366520	3%
GALR2	NIH	MRS5980	Agonist	10	682360	7%
GCGR	NIH	MRS5980	Agonist	10	277760	1%
GHSR	NIH	MRS5980	Agonist	10	448000	5%
GIPR	NIH	MRS5980	Agonist	10	14420	4%
GLP1R	NIH	MRS5980	Agonist	10	194040	1%

GPCR ID	Customer	Compound ID	Assay Mode	Conc [µM]	Mean RLU	% Activity
GLP2R	NIH	MRS5980	Agonist	10	92540	2%
GPR1	NIH	MRS5980	Agonist	10	79660	2%
GPR103	NIH	MRS5980	Agonist	10	77560	5%
GPR109A	NIH	MRS5980	Agonist	10	538440	3%
GPR109B	NIH	MRS5980	Agonist	10	303380	-1%
GPR119	NIH	MRS5980	Agonist	10	213080	2%
GPR120	NIH	MRS5980	Agonist	10	31640	4%
GPR35	NIH	MRS5980	Agonist	10	396480	9%
GPR92	NIH	MRS5980	Agonist	10	281960	8%
GRPR	NIH	MRS5980	Agonist	10	52840	0%
HCRTR1	NIH	MRS5980	Agonist	10	108220	0%
HCRTR2	NIH	MRS5980	Agonist	10	61740	0%
HRH1	NIH	MRS5980	Agonist	10	375900	0%
HRH2	NIH	MRS5980	Agonist	10	94920	3%
HRH3	NIH	MRS5980	Agonist	10	40320	-1%
HRH4	NIH	MRS5980	Agonist	10	1021580	13%
HTR1A	NIH	MRS5980	Agonist	10	1305500	2%
HTR1B	NIH	MRS5980	Agonist	10	1135260	4%
HTR1E	NIH	MRS5980	Agonist	10	32900	9%
HTR1F	NIH	MRS5980	Agonist	10	338520	2%
HTR2A	NIH	MRS5980	Agonist	10	440580	2%
HTR2C	NIH	MRS5980	Agonist	10	457240	0%
HTR3A	NIH	MRS5980	Agonist	10	1173200	2%
KISS1R	NIH	MRS5980	Agonist	10	48700	3%
LHCGR	NIH	MRS5980	Agonist	10	27300	1%
LTB4R	NIH	MRS5980	Agonist	10	127400	0%
MC1R	NIH	MRS5980	Agonist	10	11900	0%
MC3R	NIH	MRS5980	Agonist	10	15120	-1%
MC4R	NIH	MRS5980	Agonist	10	32060	-1%
MC5R	NIH	MRS5980	Agonist	10	114100	-2%
MCHR1	NIH	MRS5980	Agonist	10	40740	6%
MCHR2	NIH	MRS5980	Agonist	10	43400	-1%
MLNR	NIH	MRS5980	Agonist	10	232680	1%
MRGPRX1	NIH	MRS5980	Agonist	10	634340	-4%
MRGPRX2	NIH	MRS5980	Agonist	10	129220	-1%
MTNR1A	NIH	MRS5980	Agonist	10	61180	8%
NMBR	NIH	MRS5980	Agonist	10	60200	-1%
NMU1R	NIH	MRS5980	Agonist	10	94640	1%
NPBWR1	NIH	MRS5980	Agonist	10	62440	2%
NPBWR2	NIH	MRS5980	Agonist	10	194180	1%
NPFFR1	NIH	MRS5980	Agonist	10	149240	5%
NPSR1B	NIH	MRS5980	Agonist	10	56420	0%
NPY1R	NIH	MRS5980	Agonist	10	56280	-3%
NPY2R	NIH	MRS5980	Agonist	10	311920	1%
NTSR1	NIH	MRS5980	Agonist	10	353640	3%
OPRD1	NIH	MRS5980	Agonist	10	108360	0%
OPRK1	NIH	MRS5980	Agonist	10	45220	0%
OPRL1	NIH	MRS5980	Agonist	10	167860	0%
OPRM1	NIH	MRS5980	Agonist	10	95340	0%
OXER1	NIH	MRS5980	Agonist	10	74480	1%
OXTR	NIH	MRS5980	Agonist	10	24920	1%
P2RY1	NIH	MRS5980	Agonist	10	88200	0%
P2RY11	NIH	MRS5980	Agonist	10	54040	2%
P2RY12	NIH	MRS5980	Agonist	10	438620	5%
P2RY2	NIH	MRS5980	Agonist	10	281680	0%
P2RY4	NIH	MRS5980	Agonist	10	421680	9%
P2RY6	NIH	MRS5980	Agonist	10	317800	5%
PPYR1	NIH	MRS5980	Agonist	10	35140	1%
PRLHR	NIH	MRS5980	Agonist	10	34440	2%
PROKR1	NIH	MRS5980	Agonist	10	30800	0%
PROKR2	NIH	MRS5980	Agonist	10	10780	1%
PTAFR	NIH	MRS5980	Agonist	10	665280	-3%
PTGER2	NIH	MRS5980	Agonist	10	22400	0%
PTGER3	NIH	MRS5980	Agonist	10	281120	3%
PTGER4	NIH	MRS5980	Agonist	10	89880	2%
PTGFR	NIH	MRS5980	Agonist	10	8400	0%
PTGIR	NIH	MRS5980	Agonist	10	141680	3%
PTHR1	NIH	MRS5980	Agonist	10	100800	1%
PTHR2	NIH	MRS5980	Agonist	10	106120	1%
RXFP3	NIH	MRS5980	Agonist	10	56280	8%
SCTR	NIH	MRS5980	Agonist	10	389200	2%
SSTR1	NIH	MRS5980	Agonist	10	30520	6%
SSTR2	NIH	MRS5980	Agonist	10	8400	0%
SSTR3	NIH	MRS5980	Agonist	10	55160	1%
SSTR5	NIH	MRS5980	Agonist	10	196140	1%
TACR1	NIH	MRS5980	Agonist	10	422240	-1%
TACR2	NIH	MRS5980	Agonist	10	419160	2%
TACR3	NIH	MRS5980	Agonist	10	111300	0%
TBXA2R	NIH	MRS5980	Agonist	10	132860	1%
TRHR	NIH	MRS5980	Agonist	10	16520	1%
TSHR(L)	NIH	MRS5980	Agonist	10	4620	-3%
UTR2	NIH	MRS5980	Agonist	10	34160	4%
VIPR1	NIH	MRS5980	Agonist	10	421680	0%
VIPR2	NIH	MRS5980	Agonist	10	307720	0%

B. Compound **4** (10 µM) tested as antagonist in GPCRMax screen (167 known GPCRs). No antagonist hits were found.

GPCR ID	Customer	Compound ID	Assay Mode	Conc (µM)	Mean RLU	% Inhibition
ADCYAP1R1	NIH	MRS3980	Antagonist	10	1288700	21%
ADORA3	NIH	MRS3980	Antagonist	10	559300	-111%
ADRA1B	NIH	MRS3980	Antagonist	10	1276320	-3%
ADRA2A	NIH	MRS3980	Antagonist	10	1091160	1%
ADRA2B	NIH	MRS3980	Antagonist	10	618940	-9%
ADRA2C	NIH	MRS3980	Antagonist	10	659120	13%
ADRB1	NIH	MRS3980	Antagonist	10	904400	-6%
ADRB2	NIH	MRS3980	Antagonist	10	760200	-1%
AGTR1	NIH	MRS3980	Antagonist	10	2631720	1%
AGTRL1	NIH	MRS3980	Antagonist	10	2088240	-2%
AVPR1A	NIH	MRS3980	Antagonist	10	343560	9%
AVPR1B	NIH	MRS3980	Antagonist	10	238840	7%
AVPR2	NIH	MRS3980	Antagonist	10	2917880	3%
BDKRB1	NIH	MRS3980	Antagonist	10	121380	-6%
BDKRB2	NIH	MRS3980	Antagonist	10	2805040	20%
BRS3	NIH	MRS3980	Antagonist	10	2652860	-11%
C3AR1	NIH	MRS3980	Antagonist	10	1875440	8%
C5AR1	NIH	MRS3980	Antagonist	10	1472520	-6%
C5L2	NIH	MRS3980	Antagonist	10	814380	-17%
CALCR	NIH	MRS3980	Antagonist	10	281120	11%
CALCRL-RAMP1	NIH	MRS3980	Antagonist	10	980000	12%
CALCRL-RAMP2	NIH	MRS3980	Antagonist	10	1064000	-7%
CALCRL-RAMP3	NIH	MRS3980	Antagonist	10	1605800	11%
CALCR-RAMP2	NIH	MRS3980	Antagonist	10	791560	-11%
CALCR-RAMP3	NIH	MRS3980	Antagonist	10	32480	-27%
CCKAR	NIH	MRS3980	Antagonist	10	1056300	3%
CCKBR	NIH	MRS3980	Antagonist	10	2899260	12%
CCR10	NIH	MRS3980	Antagonist	10	876960	-6%
CCR1	NIH	MRS3980	Antagonist	10	1194200	1%
CCR2	NIH	MRS3980	Antagonist	10	833660	-7%
CCR3	NIH	MRS3980	Antagonist	10	309120	-1%
CCR4	NIH	MRS3980	Antagonist	10	1435140	9%
CCR5	NIH	MRS3980	Antagonist	10	1087240	6%
CCR6	NIH	MRS3980	Antagonist	10	1416240	0%
CCR7	NIH	MRS3980	Antagonist	10	3297140	5%
CCR8	NIH	MRS3980	Antagonist	10	612080	7%
CCR9	NIH	MRS3980	Antagonist	10	858340	-2%
CHRM1	NIH	MRS3980	Antagonist	10	2259320	23%
CHRM2	NIH	MRS3980	Antagonist	10	687820	17%
CHRM3	NIH	MRS3980	Antagonist	10	500220	19%
CHRM4	NIH	MRS3980	Antagonist	10	992600	5%
CHRM5	NIH	MRS3980	Antagonist	10	2344860	13%
CMKLR1	NIH	MRS3980	Antagonist	10	2542820	-3%
CNR1	NIH	MRS3980	Antagonist	10	280980	1%
CNR2	NIH	MRS3980	Antagonist	10	468440	1%
CRHR1	NIH	MRS3980	Antagonist	10	3184160	14%
CRHR2	NIH	MRS3980	Antagonist	10	2728460	8%
CRTH2	NIH	MRS3980	Antagonist	10	794920	4%
CX3CR1	NIH	MRS3980	Antagonist	10	3324440	-6%
CXCR1	NIH	MRS3980	Antagonist	10	2163700	5%
CXCR2	NIH	MRS3980	Antagonist	10	903700	9%
CXCR3	NIH	MRS3980	Antagonist	10	1182160	0%
CXCR4	NIH	MRS3980	Antagonist	10	131040	5%
CXCR5	NIH	MRS3980	Antagonist	10	1065340	1%
CXCR6	NIH	MRS3980	Antagonist	10	116760	12%
CXCR7	NIH	MRS3980	Antagonist	10	1840160	13%
DRD1	NIH	MRS3980	Antagonist	10	873460	-3%
DRD2L	NIH	MRS3980	Antagonist	10	389340	-9%
DRD2S	NIH	MRS3980	Antagonist	10	1482880	-16%
DRD3	NIH	MRS3980	Antagonist	10	1025220	-3%
DRD4	NIH	MRS3980	Antagonist	10	44800	-8%
DRD5	NIH	MRS3980	Antagonist	10	366940	2%
EBI2	NIH	MRS3980	Antagonist	10	1672580	16%
EDG1	NIH	MRS3980	Antagonist	10	882840	21%
EDG3	NIH	MRS3980	Antagonist	10	4259900	-25%
EDG4	NIH	MRS3980	Antagonist	10	360640	2%
EDG5	NIH	MRS3980	Antagonist	10	1712900	11%
EDG6	NIH	MRS3980	Antagonist	10	786800	-6%
EDG7	NIH	MRS3980	Antagonist	10	680960	13%
EDNRA	NIH	MRS3980	Antagonist	10	424760	-6%
EDNRB	NIH	MRS3980	Antagonist	10	1435840	-4%
F2R	NIH	MRS3980	Antagonist	10	1251600	-7%
F2RL1	NIH	MRS3980	Antagonist	10	2717680	0%
F2RL3	NIH	MRS3980	Antagonist	10	2605340	-6%
FFAR1	NIH	MRS3980	Antagonist	10	420420	21%
FPR1	NIH	MRS3980	Antagonist	10	3263920	-8%
FPRL1	NIH	MRS3980	Antagonist	10	2497880	1%
FSHR	NIH	MRS3980	Antagonist	10	553700	-11%
GALR1	NIH	MRS3980	Antagonist	10	2130820	2%
GALR2	NIH	MRS3980	Antagonist	10	1271620	13%
GCGR	NIH	MRS3980	Antagonist	10	2070180	8%
GHSR	NIH	MRS3980	Antagonist	10	1460900	-4%
GIPR	NIH	MRS3980	Antagonist	10	77980	-8%
GLP1R	NIH	MRS3980	Antagonist	10	2057720	-6%

GPCR ID	Customer	Compound ID	Assay Mode	Conc (µM)	Mean RLU	% Inhibition
GLP2R	NIH	MRS3980	Antagonist	10	728840	-7%
GPR1	NIH	MRS3980	Antagonist	10	973280	-2%
GPR103	NIH	MRS3980	Antagonist	10	148120	1%
GPR109A	NIH	MRS3980	Antagonist	10	1302700	5%
GPR109B	NIH	MRS3980	Antagonist	10	2364040	-7%
GPR119	NIH	MRS3980	Antagonist	10	311780	9%
GPR120	NIH	MRS3980	Antagonist	10	119840	20%
GPR35	NIH	MRS3980	Antagonist	10	1074360	-7%
GPR92	NIH	MRS3980	Antagonist	10	745220	26%
GRPR	NIH	MRS3980	Antagonist	10	1143900	2%
HCRTR1	NIH	MRS3980	Antagonist	10	3115420	5%
HCRTR2	NIH	MRS3980	Antagonist	10	2979620	2%
HRH1	NIH	MRS3980	Antagonist	10	1859200	-3%
HRH2	NIH	MRS3980	Antagonist	10	295260	14%
HRH3	NIH	MRS3980	Antagonist	10	299040	-11%
HRH4	NIH	MRS3980	Antagonist	10	2083460	3%
HTR1A	NIH	MRS3980	Antagonist	10	2051280	27%
HTR1B	NIH	MRS3980	Antagonist	10	2161600	9%
HTR1E	NIH	MRS3980	Antagonist	10	61320	12%
HTR1F	NIH	MRS3980	Antagonist	10	725340	16%
HTR2A	NIH	MRS3980	Antagonist	10	1747060	17%
HTR2C	NIH	MRS3980	Antagonist	10	1963040	11%
HTR5A	NIH	MRS3980	Antagonist	10	3366160	11%
KISS1R	NIH	MRS3980	Antagonist	10	222460	-3%
LHCGR	NIH	MRS3980	Antagonist	10	157920	-1%
LTB4R	NIH	MRS3980	Antagonist	10	1601460	0%
MC1R	NIH	MRS3980	Antagonist	10	41720	-6%
MC3R	NIH	MRS3980	Antagonist	10	83020	15%
MC4R	NIH	MRS3980	Antagonist	10	191380	-1%
MC5R	NIH	MRS3980	Antagonist	10	356020	0%
MCHR1	NIH	MRS3980	Antagonist	10	126000	-7%
MCHR2	NIH	MRS3980	Antagonist	10	268940	22%
MLNR	NIH	MRS3980	Antagonist	10	2167620	-1%
MRGPRX1	NIH	MRS3980	Antagonist	10	2476880	6%
MRGPRX2	NIH	MRS3980	Antagonist	10	741020	5%
MTNR1A	NIH	MRS3980	Antagonist	10	158900	-16%
NMBR	NIH	MRS3980	Antagonist	10	757820	9%
NMU1R	NIH	MRS3980	Antagonist	10	1184540	3%
NPBWR1	NIH	MRS3980	Antagonist	10	167860	10%
NPBWR2	NIH	MRS3980	Antagonist	10	1376900	-4%
NPFFR1	NIH	MRS3980	Antagonist	10	386260	-8%
NPSR1B	NIH	MRS3980	Antagonist	10	428400	3%
NPY1R	NIH	MRS3980	Antagonist	10	582820	12%
NPY2R	NIH	MRS3980	Antagonist	10	2774940	-2%
NTSR1	NIH	MRS3980	Antagonist	10	1710380	-1%
OPRD1	NIH	MRS3980	Antagonist	10	582680	7%
OPRK1	NIH	MRS3980	Antagonist	10	227220	-10%
OPRL1	NIH	MRS3980	Antagonist	10	885360	26%
OPRM1	NIH	MRS3980	Antagonist	10	2581880	0%
OXER1	NIH	MRS3980	Antagonist	10	222180	-15%
OXTR	NIH	MRS3980	Antagonist	10	451640	-5%
P2RY1	NIH	MRS3980	Antagonist	10	322980	6%
P2RY11	NIH	MRS3980	Antagonist	10	373660	2%
P2RY12	NIH	MRS3980	Antagonist	10	1568140	22%
P2RY2	NIH	MRS3980	Antagonist	10	1186360	-6%
P2RY4	NIH	MRS3980	Antagonist	10	1128260	4%
P2RY6	NIH	MRS3980	Antagonist	10	1559880	8%
PPYR1	NIH	MRS3980	Antagonist	10	523460	-2%
PRLHR	NIH	MRS3980	Antagonist	10	160720	-7%
PROKR1	NIH	MRS3980	Antagonist	10	490560	14%
PROKR2	NIH	MRS3980	Antagonist	10	177380	-12%
PTAFR	NIH	MRS3980	Antagonist	10	3483200	10%
PTGER2	NIH	MRS3980	Antagonist	10	108780	-3%
PTGER3	NIH	MRS3980	Antagonist	10	1172640	1%
PTGER4	NIH	MRS3980	Antagonist	10	771540	2%
PTGFR	NIH	MRS3980	Antagonist	10	324100	3%
PTGIR	NIH	MRS3980	Antagonist	10	500220	-1%
PTHR1	NIH	MRS3980	Antagonist	10	2466380	3%
PTHR2	NIH	MRS3980	Antagonist	10	2658460	1%
RXFP3	NIH	MRS3980	Antagonist	10	195020	-21%
SCTR	NIH	MRS3980	Antagonist	10	2167060	6%
SSTR1	NIH	MRS3980	Antagonist	10	60200	-8%
SSTR2	NIH	MRS3980	Antagonist	10	593180	-16%
SSTR3	NIH	MRS3980	Antagonist	10	617680	6%
SSTR5	NIH	MRS3980	Antagonist	10	858480	-4%
TACR1	NIH	MRS3980	Antagonist	10	3467800	5%
TACR2	NIH	MRS3980	Antagonist	10	1940400	-8%
TACR3	NIH	MRS3980	Antagonist	10	2155720	3%
TBXA2R	NIH	MRS3980	Antagonist	10	921340	-6%
TRHR	NIH	MRS3980	Antagonist	10	349720	-1%
TSHR(L)	NIH	MRS3980	Antagonist	10	44940	-1%
UTR2	NIH	MRS3980	Antagonist	10	131180	-8%
VIPR1	NIH	MRS3980	Antagonist	10	3254440	-5%
VIPR2	NIH	MRS3980	Antagonist	10	3901240	1%

C. Compound **4** (10 μM) tested as agonist in a screen of 73 orphan GPCRs (OrphanMAX). No agonist hits were found. Compounds were tested at the concentration shown in the table. Basal control activity is given. Raw activity (RLU units) of individual replicates and mean RLU and percentage activity are shown. Percentage activity was calculated relative to the basal activity for each orphan GPCR target.

GPCR ID	Customer	Baseline Vehicle	Mean RLU	SD	%CV	Compound ID	Assay Mode	Test Conc (μM)	Rep 1 RLU	Rep 2 RLU	Mean RLU	SD	%CV	% Activity
BAI1	NIH	DMSO	119665	12304	10%	MRS5980	Agonist	10	116760	118160	117460	990	1%	-2%
BAI2	NIH	DMSO	206710	9061	4%	MRS5980	Agonist	10	211400	206080	208740	3762	2%	1%
BAI3	NIH	DMSO	133823	9532	7%	MRS5980	Agonist	10	127400	122360	124880	3564	3%	-7%
CCRL2	NIH	DMSO	17815	1942	11%	MRS5980	Agonist	10	15120	15400	15260	198	1%	-14%
DARC	NIH	DMSO	226135	17207	8%	MRS5980	Agonist	10	199080	193200	196140	4158	2%	-13%
GHSR1B	NIH	DMSO	161595	2641	2%	MRS5980	Agonist	10	151200	144200	147700	4950	3%	-9%
GPR101	NIH	DMSO	169733	11857	7%	MRS5980	Agonist	10	148680	149520	149100	594	0%	-12%
GPR107	NIH	DMSO	1621900	89951	6%	MRS5980	Agonist	10	1423800	1483720	1453760	42370	3%	-10%
GPR12	NIH	DMSO	85190	4063	5%	MRS5980	Agonist	10	81760	83440	82600	1188	1%	-3%
GPR123	NIH	DMSO	3536540	143811	4%	MRS5980	Agonist	10	3592120	3557960	3575040	24155	1%	1%
GPR132	NIH	DMSO	1586900	178177	11%	MRS5980	Agonist	10	1206240	1182160	1194200	17027	1%	-25%
GPR135	NIH	DMSO	36383	2710	7%	MRS5980	Agonist	10	36400	37800	37100	990	3%	2%
GPR137	NIH	DMSO	75968	4795	6%	MRS5980	Agonist	10	72800	78120	75460	3762	5%	-1%
GPR139	NIH	DMSO	1166480	55521	5%	MRS5980	Agonist	10	1168720	1086680	1127700	58011	5%	-3%
GPR141	NIH	DMSO	24378	2630	11%	MRS5980	Agonist	10	30800	24360	27580	4554	17%	13%
GPR142	NIH	DMSO	166268	16839	10%	MRS5980	Agonist	10	144760	150920	147840	4356	3%	-11%
GPR143	NIH	DMSO	172410	11103	6%	MRS5980	Agonist	10	169960	199080	184520	20591	11%	7%
GPR146	NIH	DMSO	35945	1451	4%	MRS5980	Agonist	10	38080	39200	38640	792	2%	7%
GPR148	NIH	DMSO	129133	12473	10%	MRS5980	Agonist	10	135520	118720	127120	11879	9%	-2%
GPR149	NIH	DMSO	42893	3872	9%	MRS5980	Agonist	10	38920	33040	35980	4158	12%	-16%
GPR15	NIH	DMSO	27510	2853	10%	MRS5980	Agonist	10	26040	24920	25480	792	3%	-7%
GPR150	NIH	DMSO	617610	35895	6%	MRS5980	Agonist	10	614880	579880	597380	24749	4%	-3%
GPR151	NIH	DMSO	482685	25111	5%	MRS5980	Agonist	10	455840	432040	443940	16829	4%	-8%
GPR152	NIH	DMSO	360658	16188	4%	MRS5980	Agonist	10	343280	345800	344540	1782	1%	-4%
GPR157	NIH	DMSO	2059365	181944	9%	MRS5980	Agonist	10	1662080	1601320	1631700	42964	3%	-21%
GPR161	NIH	DMSO	18130	5045	28%	MRS5980	Agonist	10	16240	14560	15400	1188	8%	-15%
GPR162	NIH	DMSO	53253	5824	11%	MRS5980	Agonist	10	45640	47880	46760	1584	3%	-12%
GPR17	NIH	DMSO	74393	5109	7%	MRS5980	Agonist	10	67200	70280	68740	2178	3%	-8%
GPR171	NIH	DMSO	259963	46637	18%	MRS5980	Agonist	10	220080	225680	222880	3960	2%	-14%
GPR173	NIH	DMSO	93660	6903	7%	MRS5980	Agonist	10	91000	82880	86940	5742	7%	-7%
GPR176	NIH	DMSO	1042825	67715	6%	MRS5980	Agonist	10	989240	978880	984060	7326	1%	-6%
GPR18	NIH	DMSO	95305	19705	21%	MRS5980	Agonist	10	81760	90440	86100	6138	7%	-10%
GPR182	NIH	DMSO	2403800	81460	3%	MRS5980	Agonist	10	2394560	2211720	2303140	129287	6%	-4%
GPR20	NIH	DMSO	48983	4320	9%	MRS5980	Agonist	10	52920	48160	50540	3366	7%	3%
GPR23	NIH	DMSO	2058823	81290	4%	MRS5980	Agonist	10	2025240	1825880	1925560	140969	7%	-6%
GPR25	NIH	DMSO	160213	8225	5%	MRS5980	Agonist	10	159880	150080	154980	6930	4%	-3%
GPR26	NIH	DMSO	147193	17454	12%	MRS5980	Agonist	10	119840	129360	124600	6732	5%	-15%
GPR27	NIH	DMSO	145723	10909	7%	MRS5980	Agonist	10	146720	141960	144340	3366	2%	-1%
GPR3	NIH	DMSO	1949430	122326	6%	MRS5980	Agonist	10	2020200	1867880	1944040	107707	6%	0%
GPR30	NIH	DMSO	749420	45689	6%	MRS5980	Agonist	10	732480	714560	723520	12671	2%	-3%
GPR31	NIH	DMSO	25200	1838	7%	MRS5980	Agonist	10	27440	23800	25620	2574	10%	2%
GPR32	NIH	DMSO	169890	7335	4%	MRS5980	Agonist	10	168000	164360	166180	2574	2%	-2%
GPR37	NIH	DMSO	2048288	164658	8%	MRS5980	Agonist	10	1756720	1648640	1702680	76424	4%	-17%
GPR37L1	NIH	DMSO	58783	5826	10%	MRS5980	Agonist	10	57680	63280	60480	3960	7%	3%
GPR39	NIH	DMSO	1036805	80353	8%	MRS5980	Agonist	10	1039920	1168720	1104320	91075	8%	7%
GPR4	NIH	DMSO	527328	78090	15%	MRS5980	Agonist	10	494200	472640	483420	15245	3%	-8%
GPR45	NIH	DMSO	1098615	59665	5%	MRS5980	Agonist	10	1142960	1061480	1102220	57615	5%	0%
GPR50	NIH	DMSO	3523503	99560	3%	MRS5980	Agonist	10	3359440	3365320	3362380	4158	0%	-5%
GPR52	NIH	DMSO	289958	22877	8%	MRS5980	Agonist	10	307720	298760	303240	6336	2%	5%
GPR55	NIH	DMSO	1709838	86214	5%	MRS5980	Agonist	10	1638560	1557080	1597820	57615	4%	-7%
GPR6	NIH	DMSO	38868	2486	6%	MRS5980	Agonist	10	41440	36680	39060	3366	9%	0%
GPR61	NIH	DMSO	352888	16556	5%	MRS5980	Agonist	10	340760	345800	343280	3564	1%	-3%
GPR65	NIH	DMSO	151060	10637	7%	MRS5980	Agonist	10	143920	122640	133280	15047	11%	-12%
GPR75	NIH	DMSO	116253	8115	7%	MRS5980	Agonist	10	96320	106400	101360	7128	7%	-13%
GPR78	NIH	DMSO	85663	5624	7%	MRS5980	Agonist	10	75600	77280	76440	1188	2%	-11%
GPR79	NIH	DMSO	138723	12178	9%	MRS5980	Agonist	10	136920	133000	134960	2772	2%	-3%
GPR83	NIH	DMSO	942183	60023	6%	MRS5980	Agonist	10	895440	821520	858480	52269	6%	-9%
GPR84	NIH	DMSO	205065	27138	13%	MRS5980	Agonist	10	213640	216440	215040	1980	1%	5%
GPR85	NIH	DMSO	433755	47056	11%	MRS5980	Agonist	10	376600	415240	395920	27323	7%	-9%
GPR88	NIH	DMSO	46130	4637	10%	MRS5980	Agonist	10	44520	40040	42280	3168	7%	-8%
GPR91	NIH	DMSO	807940	101237	13%	MRS5980	Agonist	10	798000	632520	715260	117012	16%	-11%
GPR97	NIH	DMSO	3703228	120664	3%	MRS5980	Agonist	10	3598560	3627120	3612840	20195	1%	-2%
LGR4	NIH	DMSO	28683	3564	12%	MRS5980	Agonist	10	24080	19040	21560	3564	17%	-25%
LGR5	NIH	DMSO	144165	8030	6%	MRS5980	Agonist	10	151200	135800	143500	10889	8%	0%
LGR6	NIH	DMSO	33250	4670	14%	MRS5980	Agonist	10	24360	23240	23800	792	3%	-28%
MRGPRD	NIH	DMSO	130095	7913	6%	MRS5980	Agonist	10	122640	103880	113260	13265	12%	-13%
MRGPRE	NIH	DMSO	393593	20992	5%	MRS5980	Agonist	10	384720	392560	388640	5544	1%	-1%
MRGPRF	NIH	DMSO	2059068	82876	4%	MRS5980	Agonist	10	2066120	2168880	2117500	72662	3%	3%
MRGPRX4	NIH	DMSO	221515	22553	10%	MRS5980	Agonist	10	215880	242200	229040	18611	8%	3%
OPN5	NIH	DMSO	635635	35710	6%	MRS5980	Agonist	10	604520	628600	616560	17027	3%	-3%
OXGR1	NIH	DMSO	395693	23786	6%	MRS5980	Agonist	10	401520	370160	385840	22175	6%	-2%
P2RY8	NIH	DMSO	3050040	110986	4%	MRS5980	Agonist	10	2866360	2902200	2884280	25343	1%	-5%
TAAR5	NIH	DMSO	189175	8393	4%	MRS5980	Agonist	10	172480	178920	175700	4554	3%	-7%

D. Compound **4** (10 µM) tested as antagonist in a screen of 73 orphan GPCRs (OrphanMAX).

No antagonist hits were found.

GPCR ID	Customer	Baseline Vehicle	Mean RLU	SD	%CV	Compound ID	Assay Mode	Test Conc (µM)	Rep 1 RLU	Rep 2 RLU	Mean RLU	SD	%CV	% Activity
BAI1	NIH	DMSO	119665	12304	10%	MRS7154	Agonist	10	109480	113680	111580	2970	3%	-7%
BAI2	NIH	DMSO	206710	9061	4%	MRS7154	Agonist	10	194040	186760	190400	5148	3%	-8%
BAI3	NIH	DMSO	133823	9532	7%	MRS7154	Agonist	10	105280	100800	103040	3168	3%	-23%
CCRL2	NIH	DMSO	17815	1942	11%	MRS7154	Agonist	10	15680	14280	14980	990	7%	-16%
DARC	NIH	DMSO	226135	17207	8%	MRS7154	Agonist	10	199360	194320	196840	3564	2%	-13%
GHSR1B	NIH	DMSO	161595	2641	2%	MRS7154	Agonist	10	132720	127680	130200	3564	3%	-19%
GPR101	NIH	DMSO	169733	11857	7%	MRS7154	Agonist	10	159320	153440	156380	4158	3%	-8%
GPR107	NIH	DMSO	1621900	89951	6%	MRS7154	Agonist	10	1527400	1667960	1597680	99391	6%	-1%
GPR12	NIH	DMSO	85190	4063	5%	MRS7154	Agonist	10	86800	77840	82320	6336	8%	-3%
GPR123	NIH	DMSO	3536540	143811	4%	MRS7154	Agonist	10	3665480	3863440	3764460	139979	4%	6%
GPR132	NIH	DMSO	1586900	178177	11%	MRS7154	Agonist	10	929320	875280	902300	38212	4%	-43%
GPR135	NIH	DMSO	36383	2710	7%	MRS7154	Agonist	10	48160	42560	45360	3960	9%	25%
GPR137	NIH	DMSO	75968	4795	6%	MRS7154	Agonist	10	65240	67760	66500	1782	3%	-12%
GPR139	NIH	DMSO	1166480	55521	5%	MRS7154	Agonist	10	1081640	1052240	1066940	20789	2%	-9%
GPR141	NIH	DMSO	24378	2630	11%	MRS7154	Agonist	10	24920	21560	23240	2376	10%	-5%
GPR142	NIH	DMSO	166268	16839	10%	MRS7154	Agonist	10	167720	150920	159320	11879	7%	-4%
GPR143	NIH	DMSO	172410	11103	6%	MRS7154	Agonist	10	163800	191240	177520	19403	11%	3%
GPR146	NIH	DMSO	35945	1451	4%	MRS7154	Agonist	10	32480	35280	33880	1980	6%	-6%
GPR148	NIH	DMSO	129133	12473	10%	MRS7154	Agonist	10	97160	106960	102060	6930	7%	-21%
GPR149	NIH	DMSO	42893	3872	9%	MRS7154	Agonist	10	48160	35560	41860	8910	21%	-2%
GPR15	NIH	DMSO	27510	2853	10%	MRS7154	Agonist	10	22680	23800	23240	792	3%	-16%
GPR150	NIH	DMSO	617610	35895	6%	MRS7154	Agonist	10	638120	566720	602420	50487	8%	-2%
GPR151	NIH	DMSO	482685	25111	5%	MRS7154	Agonist	10	397600	423920	410760	18611	5%	-15%
GPR152	NIH	DMSO	360658	16188	4%	MRS7154	Agonist	10	333480	357280	345380	16829	5%	-4%
GPR157	NIH	DMSO	2059365	181944	9%	MRS7154	Agonist	10	1741880	1624560	1683220	82958	5%	-18%
GPR161	NIH	DMSO	18130	5045	28%	MRS7154	Agonist	10	16520	15400	15960	792	5%	-12%
GPR162	NIH	DMSO	53253	5824	11%	MRS7154	Agonist	10	45920	42000	43960	2772	6%	-17%
GPR17	NIH	DMSO	74393	5109	7%	MRS7154	Agonist	10	72240	69440	70840	1980	3%	-5%
GPR171	NIH	DMSO	259963	46637	18%	MRS7154	Agonist	10	218120	199360	208740	13265	6%	-20%
GPR173	NIH	DMSO	93660	6903	7%	MRS7154	Agonist	10	83440	78400	80920	3564	4%	-14%
GPR176	NIH	DMSO	1042825	67715	6%	MRS7154	Agonist	10	976080	983080	979580	4950	1%	-6%
GPR18	NIH	DMSO	95305	19705	21%	MRS7154	Agonist	10	87080	82600	84840	3168	4%	-11%
GPR182	NIH	DMSO	2403800	81460	3%	MRS7154	Agonist	10	2230480	2479400	2354940	176013	7%	-2%
GPR20	NIH	DMSO	48983	4320	9%	MRS7154	Agonist	10	41720	42560	42140	594	1%	-14%
GPR23	NIH	DMSO	2058823	81290	4%	MRS7154	Agonist	10	1841280	1820560	1830920	14651	1%	-11%
GPR25	NIH	DMSO	160213	8225	5%	MRS7154	Agonist	10	151200	136920	144060	10097	7%	-10%
GPR26	NIH	DMSO	147193	17454	12%	MRS7154	Agonist	10	127960	129920	128940	1386	1%	-12%
GPR27	NIH	DMSO	145723	10909	7%	MRS7154	Agonist	10	125160	127960	126560	1980	2%	-13%
GPR3	NIH	DMSO	1949430	122326	6%	MRS7154	Agonist	10	1862560	1847720	1855140	10493	1%	-5%
GPR30	NIH	DMSO	749420	45689	6%	MRS7154	Agonist	10	711480	738920	725200	19403	3%	-3%
GPR31	NIH	DMSO	25200	1838	7%	MRS7154	Agonist	10	23240	21280	22260	1386	6%	-12%
GPR32	NIH	DMSO	169890	7335	4%	MRS7154	Agonist	10	147000	145600	146300	990	1%	-14%
GPR37	NIH	DMSO	2048288	164658	8%	MRS7154	Agonist	10	1803200	1319080	1561140	342325	22%	-24%
GPR37L1	NIH	DMSO	58783	5826	10%	MRS7154	Agonist	10	68040	57120	62580	7722	12%	6%
GPR39	NIH	DMSO	1036805	80353	8%	MRS7154	Agonist	10	1001000	1008560	1004780	5346	1%	-3%
GPR4	NIH	DMSO	527328	78090	15%	MRS7154	Agonist	10	509880	602280	556080	65337	12%	5%
GPR45	NIH	DMSO	1098615	59665	5%	MRS7154	Agonist	10	1071560	1091720	1081640	14255	1%	-2%
GPR50	NIH	DMSO	3523503	99560	3%	MRS7154	Agonist	10	3177160	3131240	3154200	32470	1%	-10%
GPR52	NIH	DMSO	289958	22877	8%	MRS7154	Agonist	10	308000	272160	290080	25343	9%	0%
GPR55	NIH	DMSO	1709838	86214	5%	MRS7154	Agonist	10	1388240	1393560	1390900	3762	0%	-19%
GPR6	NIH	DMSO	38868	2486	6%	MRS7154	Agonist	10	33040	34440	33740	990	3%	-13%
GPR61	NIH	DMSO	352888	16556	5%	MRS7154	Agonist	10	322840	339920	331380	12077	4%	-6%
GPR65	NIH	DMSO	151060	10637	7%	MRS7154	Agonist	10	148680	144200	146440	3168	2%	-3%
GPR75	NIH	DMSO	116253	8115	7%	MRS7154	Agonist	10	88480	91560	90020	2178	2%	-23%
GPR78	NIH	DMSO	85663	5624	7%	MRS7154	Agonist	10	75320	65240	70280	7128	10%	-18%
GPR79	NIH	DMSO	138723	12178	9%	MRS7154	Agonist	10	122640	133840	128240	7920	6%	-8%
GPR83	NIH	DMSO	942183	60023	6%	MRS7154	Agonist	10	763840	774760	769300	7722	1%	-18%
GPR84	NIH	DMSO	205065	27138	13%	MRS7154	Agonist	10	220360	201600	210980	13265	6%	3%
GPR85	NIH	DMSO	433755	47056	11%	MRS7154	Agonist	10	402920	402080	402500	594	0%	-7%
GPR88	NIH	DMSO	46130	4637	10%	MRS7154	Agonist	10	45640	41720	43680	2772	6%	-5%
GPR91	NIH	DMSO	807940	101237	13%	MRS7154	Agonist	10	714280	696640	705460	12473	2%	-13%
GPR97	NIH	DMSO	3703228	120664	3%	MRS7154	Agonist	10	3541160	3641680	3591420	71078	2%	-3%
LGR4	NIH	DMSO	28683	3564	12%	MRS7154	Agonist	10	23520	22400	22960	792	3%	-20%
LGR5	NIH	DMSO	144165	8030	6%	MRS7154	Agonist	10	124040	124040	124040	0	0%	-14%
LGR6	NIH	DMSO	33250	4670	14%	MRS7154	Agonist	10	26040	27160	26600	792	3%	-20%
MRGPRD	NIH	DMSO	130095	7913	6%	MRS7154	Agonist	10	106400	109200	107800	1980	2%	-17%
MRGPRE	NIH	DMSO	393593	20992	5%	MRS7154	Agonist	10	376040	388080	382060	8514	2%	-3%
MRGPRF	NIH	DMSO	2059068	82876	4%	MRS7154	Agonist	10	1794520	1973160	1883840	126318	7%	-9%
MRGPRX4	NIH	DMSO	221515	22553	10%	MRS7154	Agonist	10	148400	188440	168420	28313	17%	-24%
OPN5	NIH	DMSO	635635	35710	6%	MRS7154	Agonist	10	664720	698600	681660	23957	4%	7%
OXGR1	NIH	DMSO	395693	23786	6%	MRS7154	Agonist	10	360360	367080	363720	4752	1%	-8%
P2RY8	NIH	DMSO	3050040	110986	4%	MRS7154	Agonist	10	2687440	2846480	2766960	112458	4%	-9%
TAAR5	NIH	DMSO	189175	8393	4%	MRS7154	Agonist	10	168280	148960	158620	13661	9%	-16%

Figure S8. Compound **4** (MRS5980, 10 μM) tested as inhibitor in KinomeSCAN screen (DiscoverX).

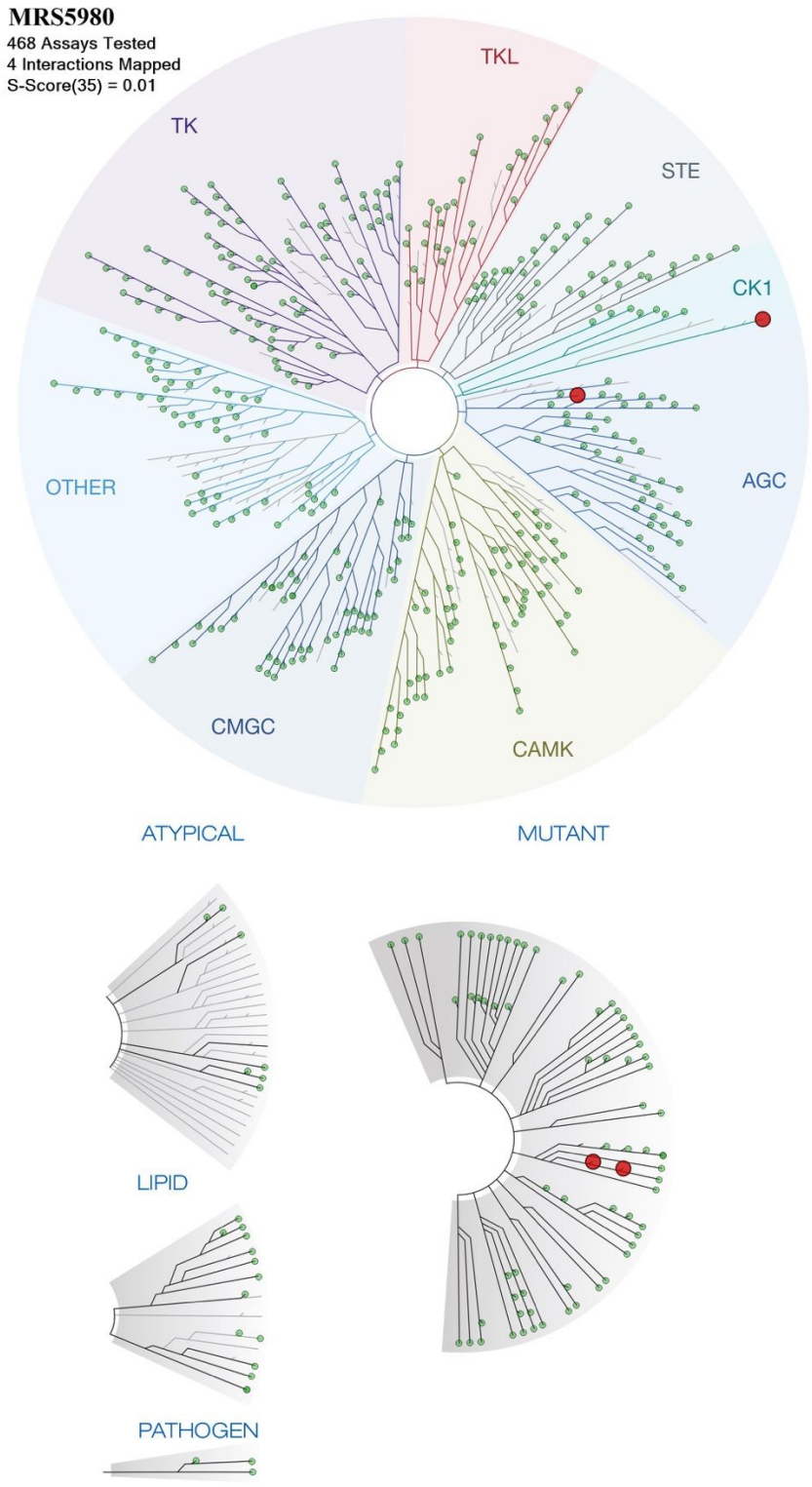

Four weak kinase screening hits (among 403 nonmutant kinases and 63 other kinases) were detected with <50% activity remaining (% inhibition at 10 μM **4**): FLT3 (ITD, D835V), 70%; LATS2, 74%; VRK2, 69%. The overall selectivity score was 0.005. All other kinases had >50% activity remaining.

Representative NMR and Mass Spectra and HPLC Analysis

(All NMR spectra were measured using CD_3OD as solvent.)

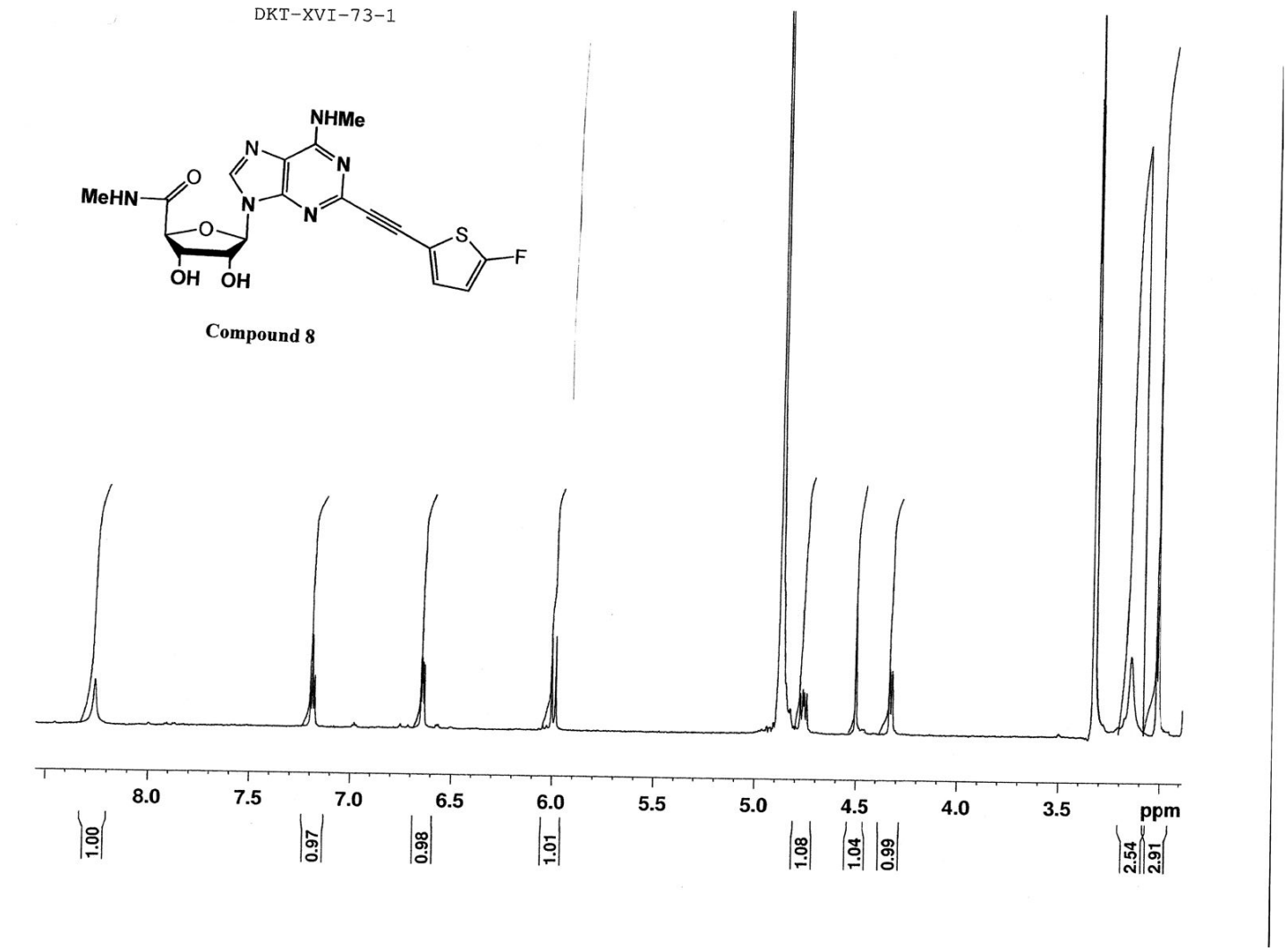

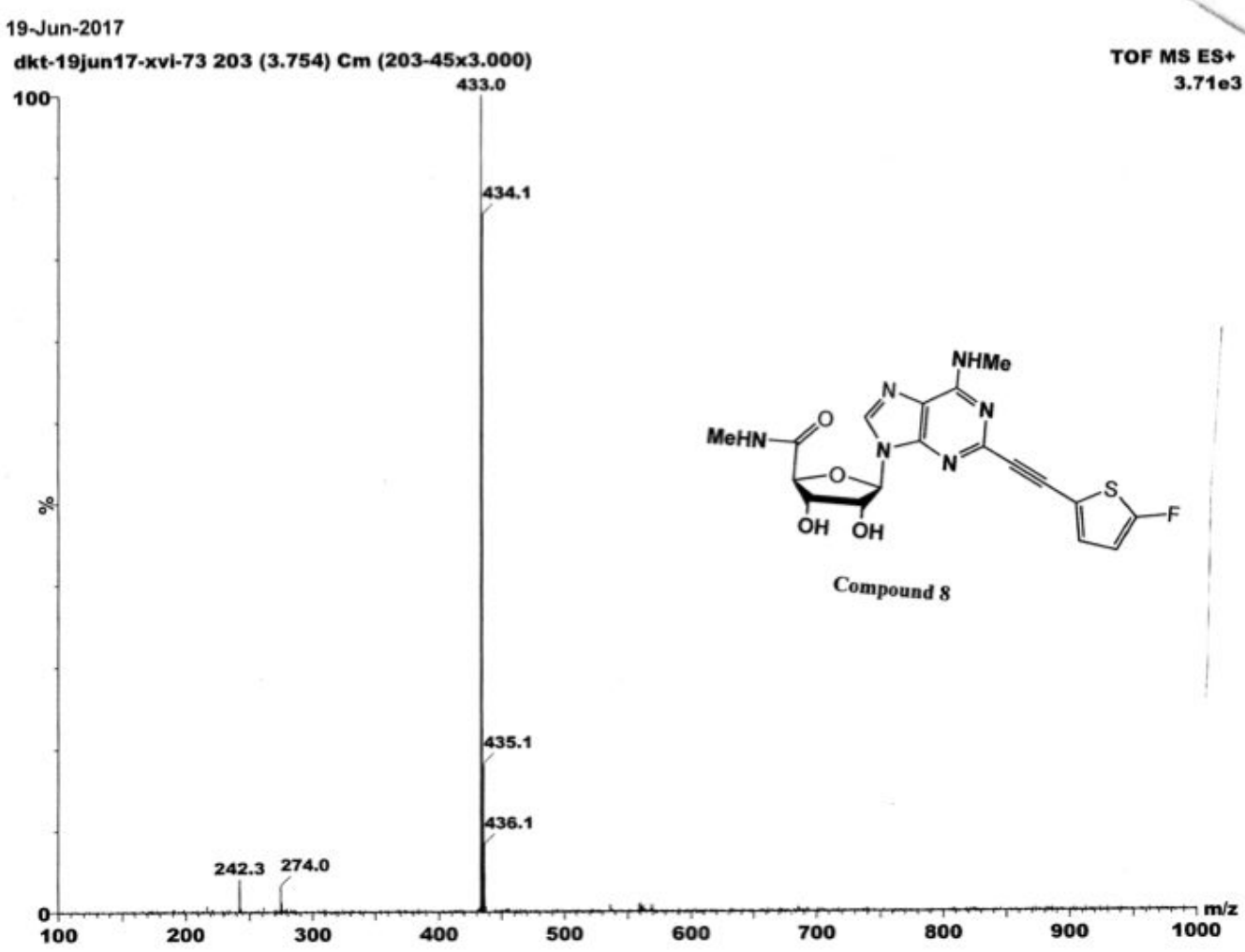
19-Jun-2017
dkt-19jun17-xvi-73 203 (3.754) Cm (203-45x3.000)
TOF MS ES+
3.71e3
100
%
0
433.0
434.1
435.1
436.1
242.3
274.0
100
200
300
400
500
600
700
800
900
1000
m/z
NHMe
MeHN
O
N
N
N
N
O
OH
OH
S
F

Compound 8

Elemental Composition Report

Single Mass Analysis
Tolerance = 10.0 mDa / DBE: min = -2.0, max = 1000.0
Element prediction: Off
Number of isotope peaks used for i-FIT = 3

Monoisotopic Mass, Even Electron Ions
60 formula(e) evaluated with 3 results within limits (up to 19 closest results for each mass)
Elements Used:
C: 0-40 H: 0-200 N: 6-6 O: 0-40 F: 1-1 32S: 1-1

19-Jun-2017
dkt-19jun17-xvi-73 207 (3.828) Cn (Cen,5, 50.00, Ar); Sm (SG, 3x5.00); Sb (12,5.00)

TOF MS ES+
6.95e+003

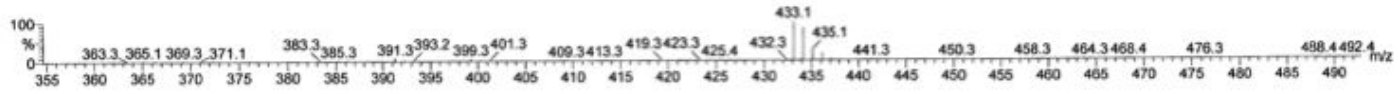

Minimum:				-2.0		
Maximum:		10.0	10.0	1000.0		
Mass	Calc. Mass	mDa	PPM	DBE	i-FIT	Formula
433.1096	433.1094	0.2	0.5	12.5	2171.8	C18 H18 N6 O4 F 32S
	433.1153	-5.7	-13.2	3.5	2645.1	C11 H22 N6 O9 F 32S
	433.1000	9.6	22.2	-0.5	2957.0	C7 H22 N6 O12 F 32S

DKT-XVI-58

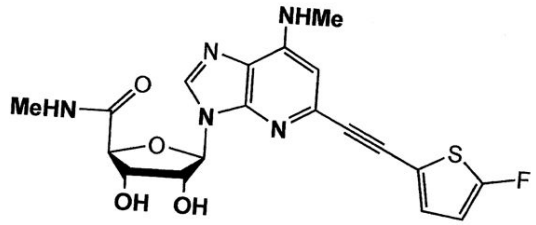

Compound 10

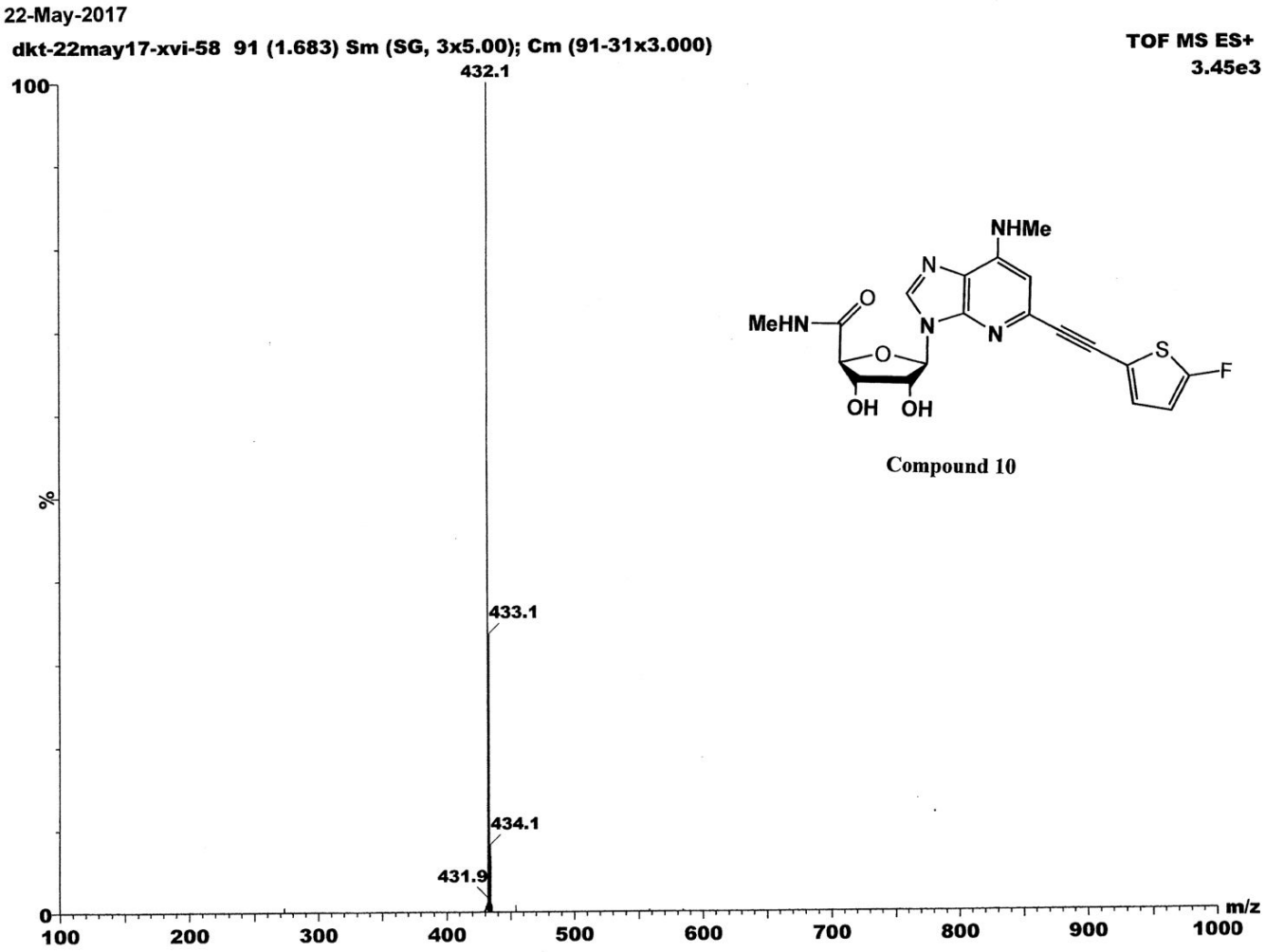
22-May-2017
dkt-22may17-xvi-58 91 (1.683) Sm (SG, 3x5.00); Cm (91-31x3.000)
TOF MS ES+
3.45e3
100
%
0
432.1
433.1
434.1
431.9
100
200
300
400
500
600
700
800
900
1000
m/z
NHMe
N
MeHN
O
N
N
O
S
F
OH
OH

Compound 10

...al Composition Report

Single Mass Analysis
Tolerance = 10.0 mDa / DBE: min = -2.0, max = 1000.0
Element prediction: Off
Number of isotope peaks used for i-FIT = 3

Monoisotopic Mass, Even Electron Ions
68 formula(e) evaluated with 3 results within limits (up to 19 closest results for each mass)
Elements Used:
C: 0-100 H: 0-200 N: 5-5 O: 0-30 F: 1-1 32S: 1-1
22-May-2017
dkl-22may17-xvi-58 97 (1.794) Cn (Cen,5, 50.00, Ar); Sm (SG, 3x5.00); Sb (12,5.00)

TOF MS ES+
4.73e+003

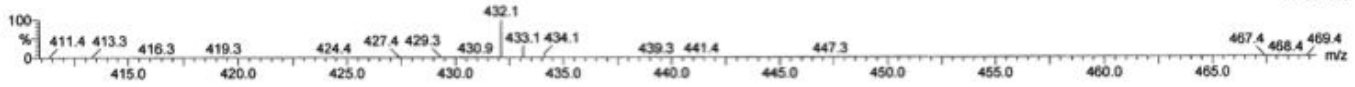

Minimum:				-2.0		
Maximum:		10.0	10.0	1000.0		
Mass	Calc. Mass	mDa	PPM	DBE	i-FIT	Formula
432.1141	432.1142	-0.1	-0.2	12.5	135.0	C19 H19 N5 O4 F 32S
	432.1201	-6.0	-13.9	3.5	268.8	C12 H23 N5 O9 F 32S
	432.1048	9.3	21.5	-0.5	393.0	C8 H23 N5 O12 F 32S

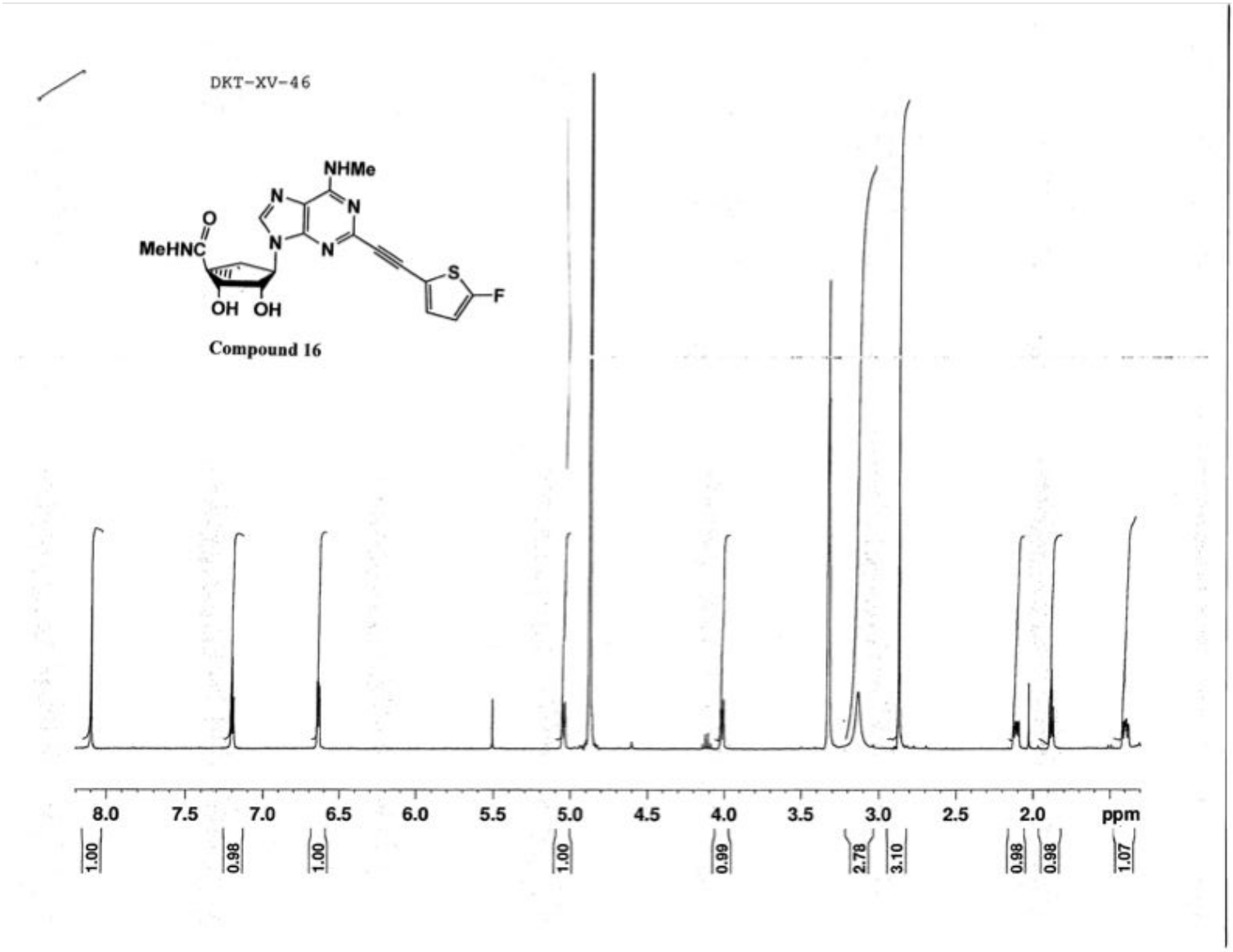
DKT-XV-46
NHMe
N
N
N
N
O
MeHNC
OH OH
S
F
Compound 16
8.0
7.5
7.0
6.5
6.0
5.5
5.0
4.5
4.0
3.5
3.0
2.5
2.0
ppm
1.00
0.98
1.00
1.00
0.99
2.78
3.10
0.98
0.98
1.07

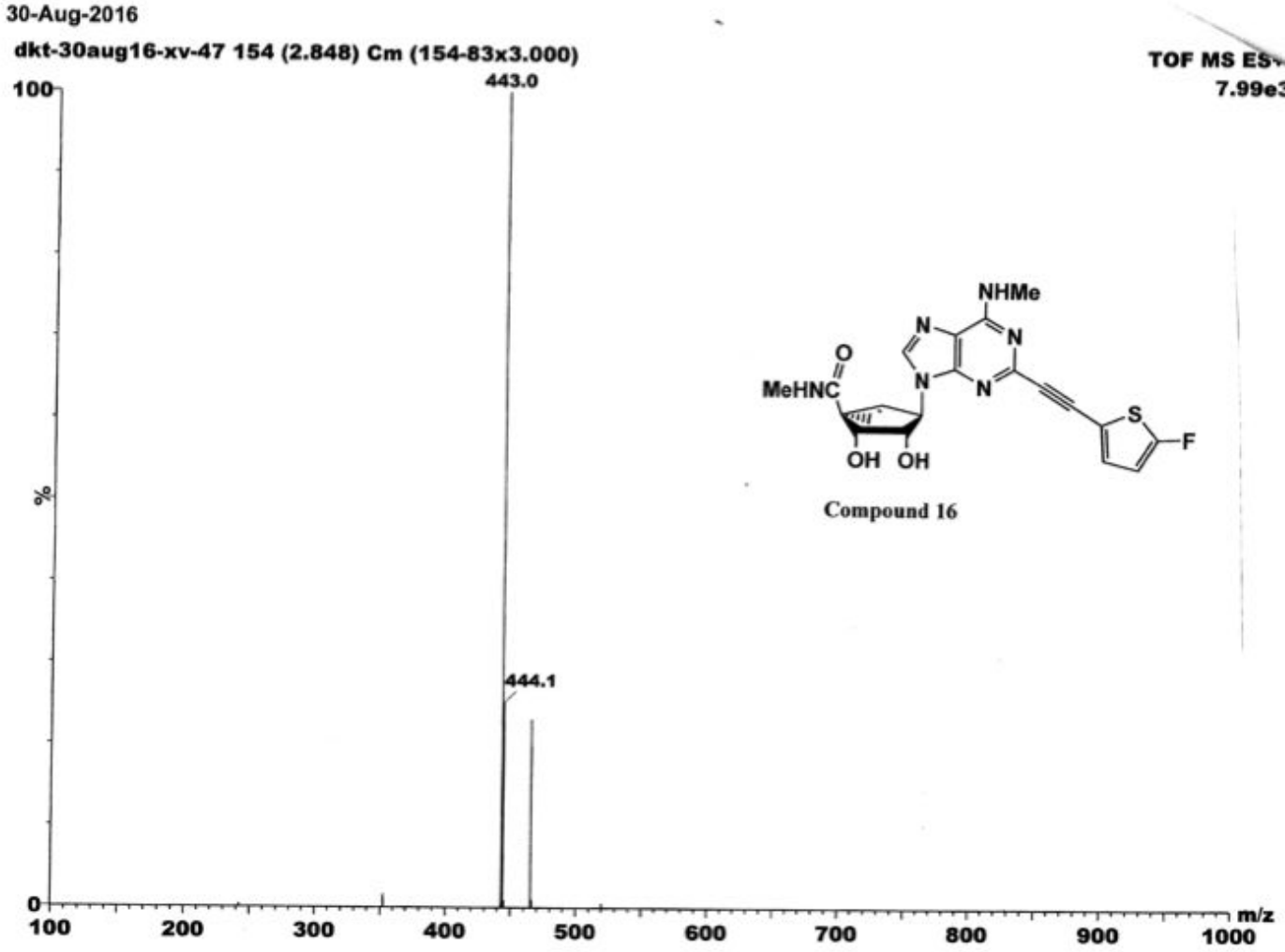
30-Aug-2016
dkt-30aug16-xv-47 154 (2.848) Cm (154-83x3.000)
TOF MS ES
7.99e3
443.0
444.1
100
%
0
100
200
300
400
500
600
700
800
900
1000
m/z
NHMe
N
N
N
N
O
MeHNC
OH OH
S
F

Compound 16

Elemental Composition Report

Single Mass Analysis
Tolerance = 10.0 mDa / DBE: min = -2.0, max = 1000.0
Element prediction: Off
Number of isotope peaks used for i-FIT = 3

Monoisotopic Mass, Even Electron Ions
66 formula(e) evaluated with 3 results within limits (up to 19 closest results for each mass)
Elements Used:
C: 0-100 H: 0-200 N: 6-6 O: 0-40 F: 1-1 32S: 1-1
30-Aug-2016
dkt-30aug16-xv-47 160 (2.959) Cn (Cen,7, 50.00, Ar); Sm (SG, 3x5.00); Sb (12,5.00)

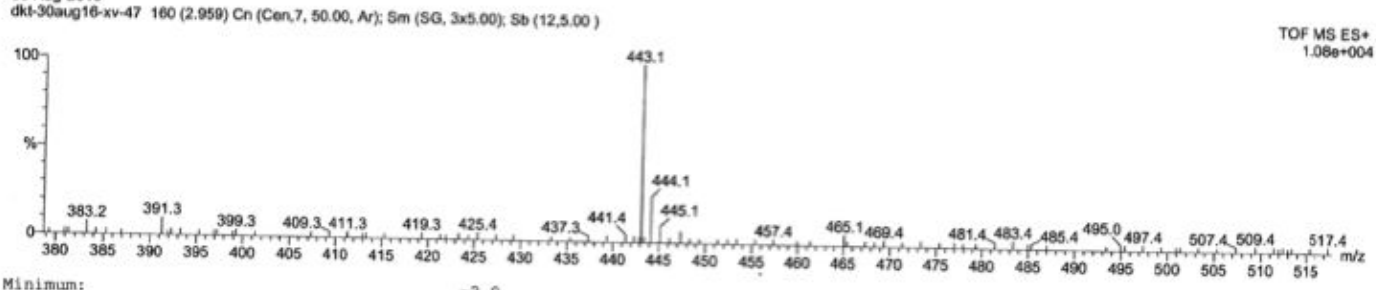

Minimum:				-2.0		
Maximum:		10.0	10.0	1000.0		
Mass	Calc. Mass	mDa	PPM	DBE	i-FIT	Formula
443.1295	443.1302	-0.7	-1.6	13.5	169.3	C20 H20 N6 O3 F 32S
	443.1360	-6.5	-14.7	4.5	317.7	C13 H24 N6 O8 F 32S
	443.1208	8.7	19.6	0.5	528.6	C9 H24 N6 O11 F 32S

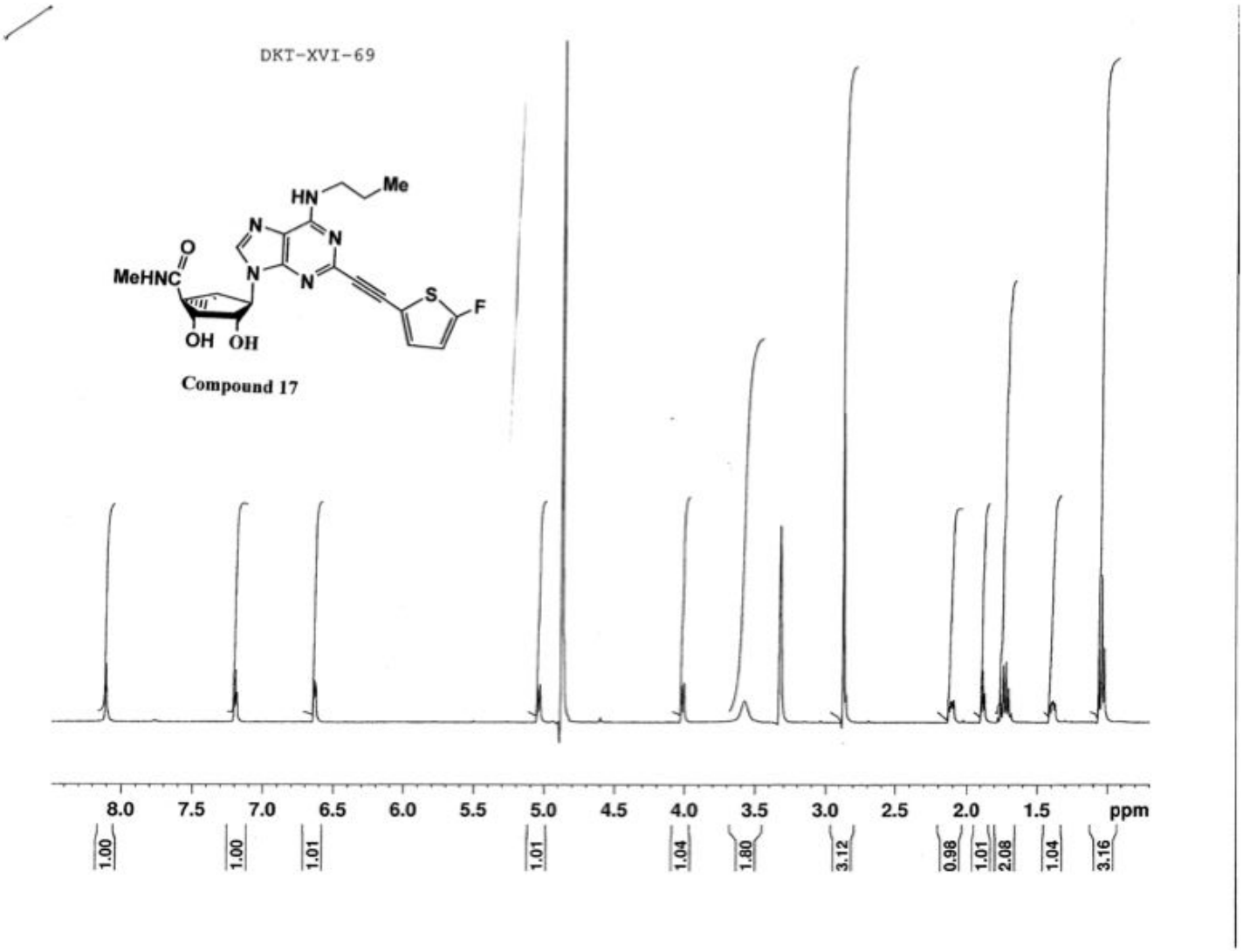
DKT-XVI-69
HN
Me
N
N
N
N
O
MeHNC
S
F
OH OH
Compound 17
8.0
7.5
7.0
6.5
6.0
5.5
5.0
4.5
4.0
3.5
3.0
2.5
2.0
1.5
ppm
1.00
1.00
1.01
1.01
1.04
1.80
3.12
0.98
1.01
2.08
1.04
3.16

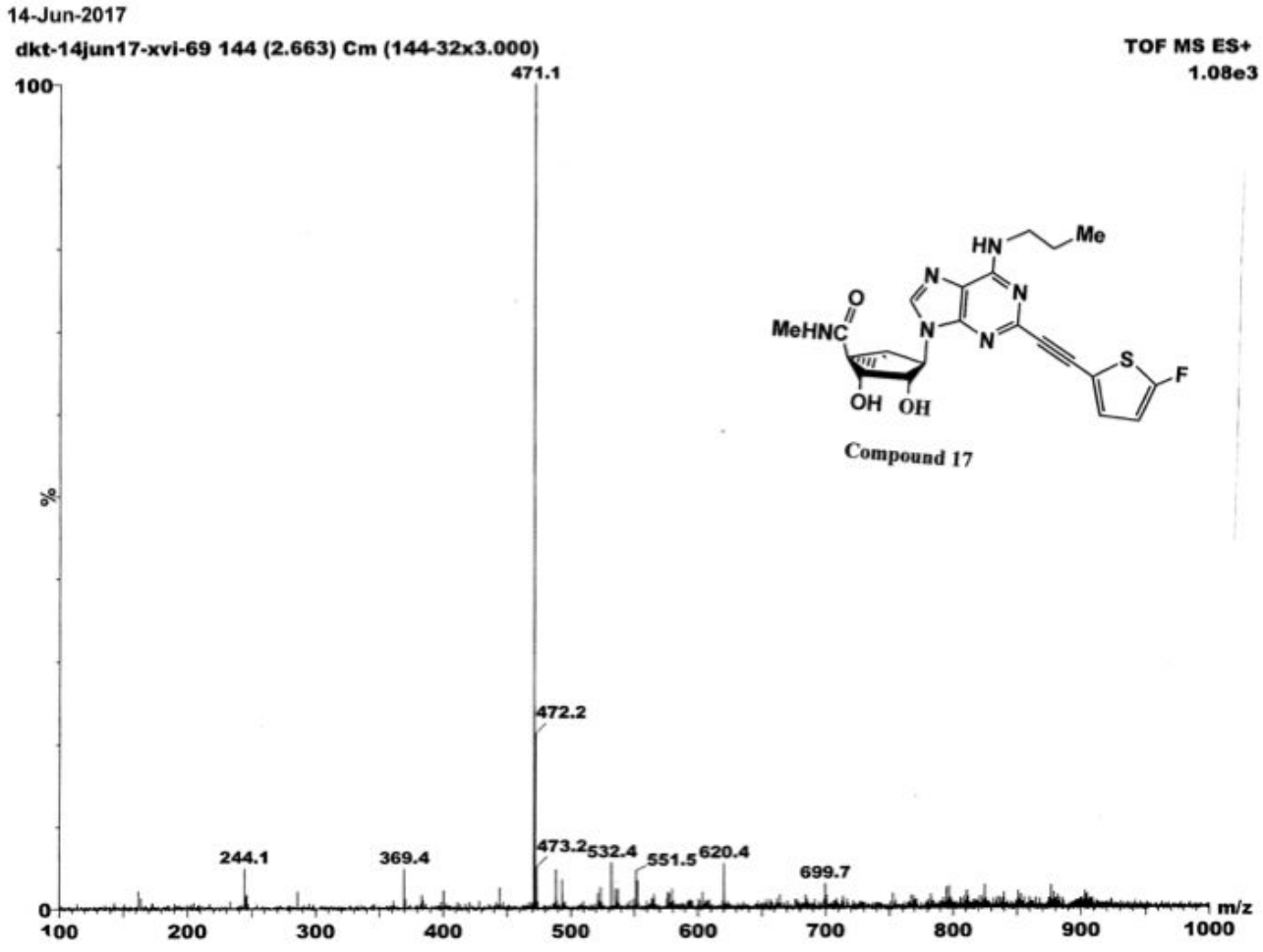
14-Jun-2017
dkt-14jun17-xvi-69 144 (2.663) Cm (144-32x3.000)
TOF MS ES+
1.08e3
100
%
0
471.1
472.2
473.2
244.1
369.4
532.4
551.5
620.4
699.7
100
200
300
400
500
600
700
800
900
1000
m/z
HN
Me
N
N
N
N
O
MeHNC
OH
OH
S
F

Compound 17

Elemental Composition Report

Single Mass Analysis
Tolerance = 20.0 mDa / DBE: min = -2.0, max = 1000.0
Element prediction: Off
Number of isotope peaks used for i-FIT = 3

Monoisotopic Mass, Even Electron Ions
76 formula(e) evaluated with 5 results within limits (up to 19 closest results for each mass)
Elements Used:
C: 0-40 H: 0-200 N: 6-6 O: 0-40 F: 1-1 32S: 1-1

14-Jun-2017
dkl-14jun17-xvi-69 141 (2.608) Cn (Cen,5, 50.00, Ar); Sm (SG, 3x5.00); Sb (12,5.00)

TOF MS ES+
5.75e+003

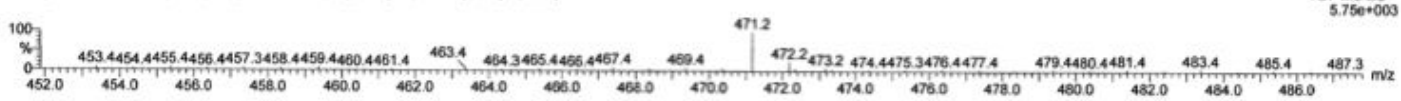

Minimum:				-2.0		
Maximum:		20.0	10.0	1000.0		
Mass	Calc. Mass	mDa	PPM	DBE	i-FIT	Formula
471.1623	471.1615	0.8	1.7	13.5	68.3	C22 H24 N6 O3 F 32S
	471.1673	-5.0	-10.6	4.5	95.1	C15 H28 N6 O8 F 32S
	471.1521	10.2	21.6	0.5	176.5	C11 H28 N6 O11 F 32S
	471.1767	-14.4	-30.6	17.5	106.5	C26 H24 N6 F 32S
	471.1462	16.1	34.2	9.5	102.7	C18 H24 N6 O6 F 32S

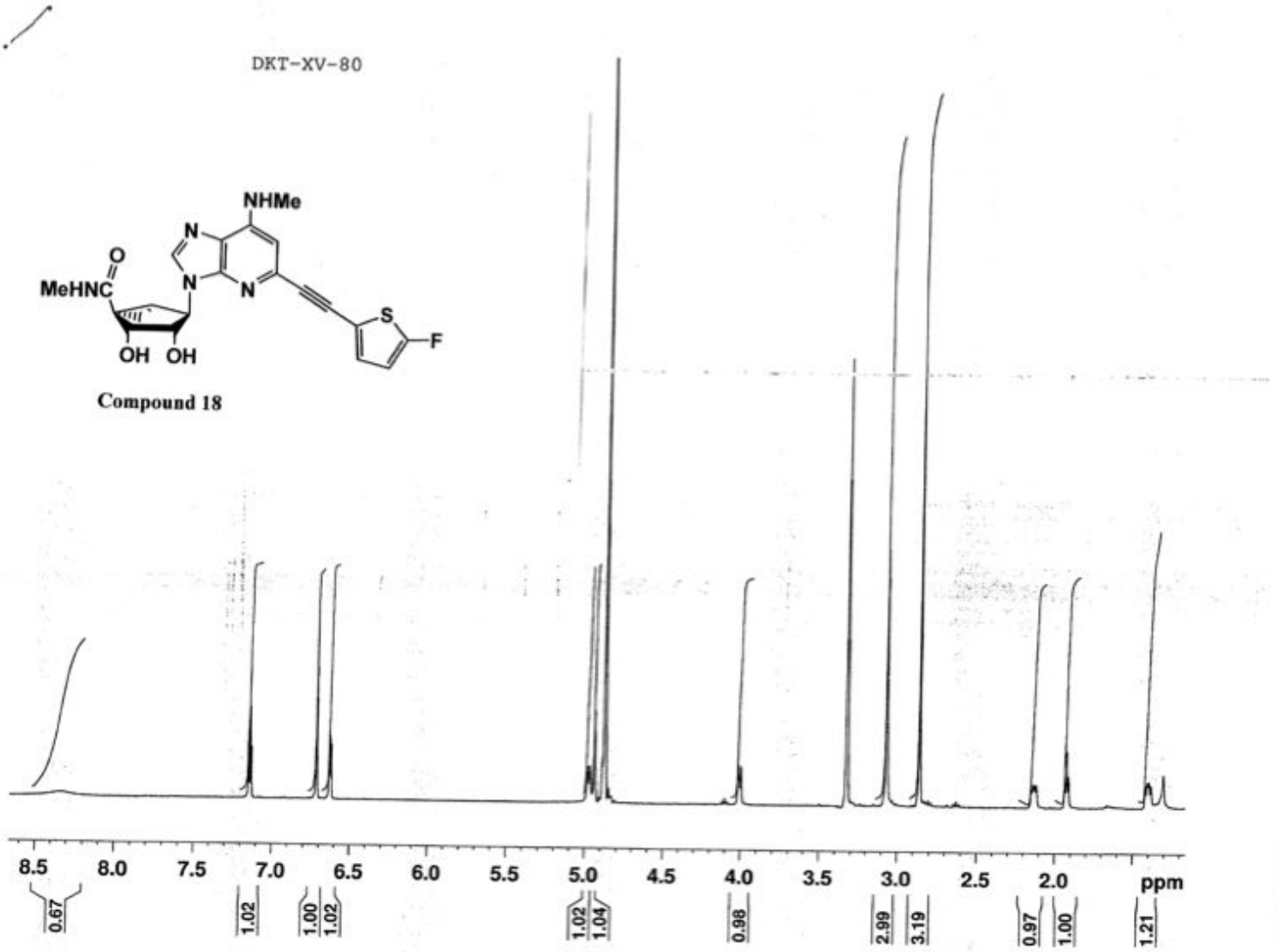
DKT-XV-80
NHMe
N
N
N
N
O
MeHNC
OH OH
S
F
Compound 18
8.5
8.0
7.5
7.0
6.5
6.0
5.5
5.0
4.5
4.0
3.5
3.0
2.5
2.0
ppm
0.67
1.02
1.00
1.02
1.02
1.04
0.98
2.99
3.19
0.97
1.00
1.21

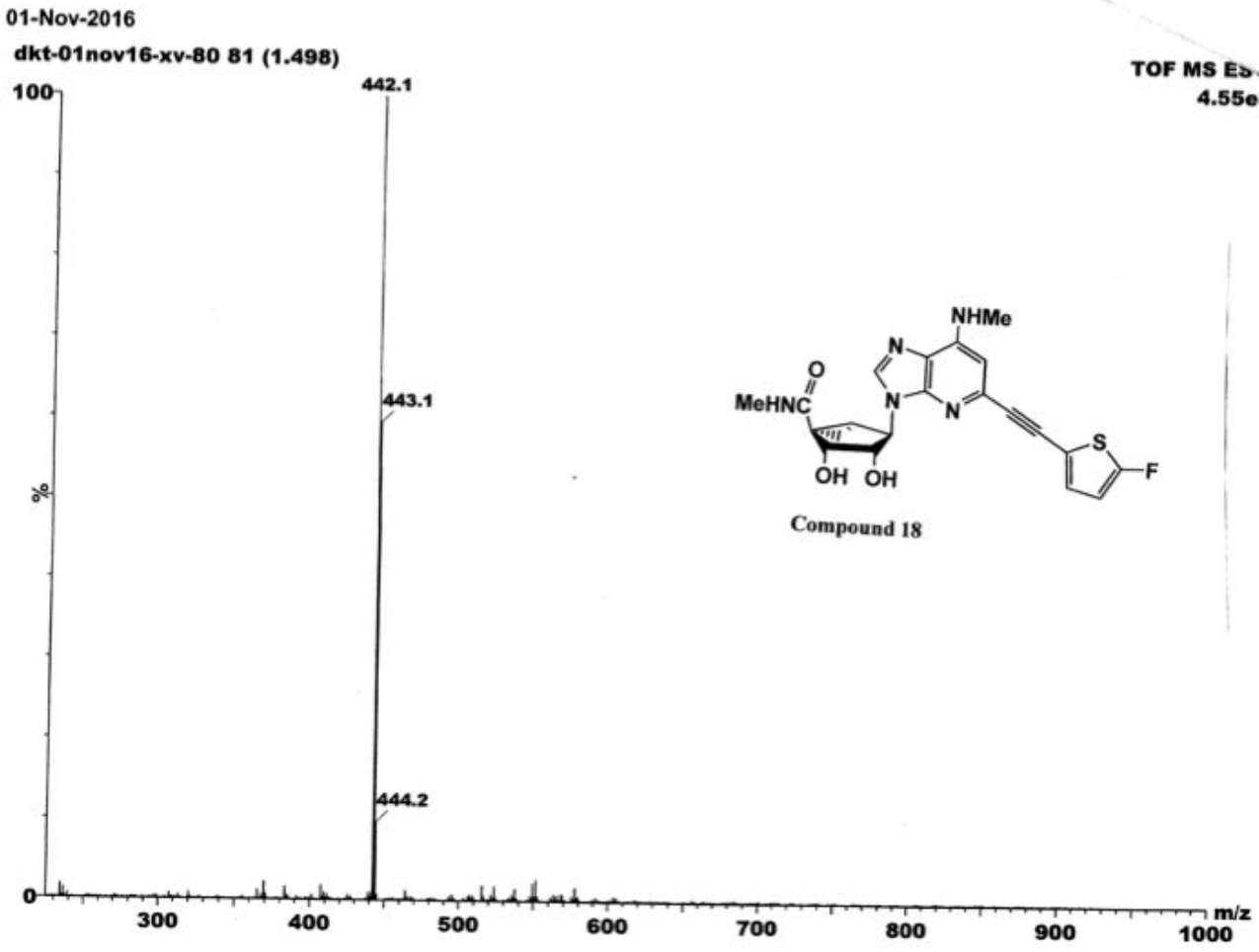
01-Nov-2016
dkt-01nov16-xv-80 81 (1.498)
TOF MS ES
4.55e3
100
%
0
442.1
443.1
444.2
300
400
500
600
700
800
900
1000
m/z
NHMe
N
O
MeHNC
N
N
N
S
F
OH OH

Compound 18

Elemental Composition Report

Single Mass Analysis
Tolerance = 10.0 mDa / DBE: min = -2.0, max = 1000.0
Element prediction: Off
Number of isotope peaks used for i-FIT = 3

Monoisotopic Mass, Even Electron Ions
67 formula(e) evaluated with 3 results within limits (up to 19 closest results for each mass)
Elements Used:
C: 0-100 H: 0-200 N: 5-5 O: 0-50 F: 1-1 32S: 1-1
01-Nov-2016
dkt-01nov16-xv-80 85 (1.572) Cn (Cen,7, 50.00, Ar); Sm (SG, 1x3.00); Sb (12,5.00)

TOF MS ES+
6.06e+003

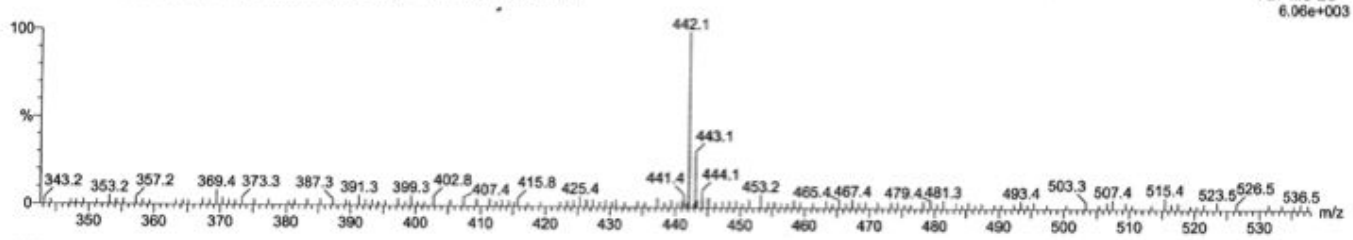

Minimum:				-2.0		
Maximum:		10.0	10.0	1000.0		
Mass	Calc. Mass	mDa	PPM	DBE	i-FIT	Formula
442.1349	442.1349	0.0	0.0	13.5	121.1	C21 H21 N5 O3 F 32S
	442.1408	-5.9	-13.3	4.5	271.5	C14 H25 N5 O8 F 32S
	442.1255	9.4	21.3	0.5	412.2	C10 H25 N5 O11 F 32S